ENPOLITE: Comparing Lithium-Ion Cells across Energy, Power, Lifetime, and Temperature

Philipp Dechent[1,2*§], Alexander Epp[1,2*], Dominik Joest[1,2], Yuliya Preger[4], Peter M. Attia[5], Weihan Li[1,2], Dirk Uwe Sauer[1,2,3]

[1]Chair for Electrochemical Energy Conversion and Storage Systems, Institute for Power Electronics and Electrical Drives (ISEA), RWTH Aachen University, Germany
[2]Jülich Aachen Research Alliance, JARA-Energy, Germany
[3]Helmholtz Institute Münster (HI MS), IEK-12, Forschungszentrum Jülich, Germany
[4]Energy Storage Technology and Systems, Sandia National Laboratories, 1515 Eubank Blvd SE, Albuquerque, New Mexico 87185, USA
[5]Department of Materials Science and Engineering, Stanford University, Stanford, California 94305, USA
* These authors contributed equally
§ Corresponding author: batteries@isea.rwth-aachen.de, Philipp.dechent@isea.rwth-aachen.de

Abstract: Lithium-Ion battery lifetimes from cyclic and calendar aging tests of more than 1000 cells were compared employing novel plots termed ENPOLITE (**en**ergy-**po**wer-**li**fetime-**te**mperature). Battery cell data from in-house measurements and published data were combined into a uniform database; the total dataset size exceeds 1000 GB. At a glance, ENPOLITE plots inform about the nominal capacity, cell format, cell chemistry, average aging test duration, measurement temperature, specific power employed for testing, energy density, and the achieved lifetime for every cell. A battery lifetime coefficient was derived, allowing the comparison of lithium-ion batteries with different weights or volumes, capacities, and cell chemistries. The combination of multiple parameters in ENPOLITE facilitated a thorough comparison of various batteries' respective lifetimes. In addition to the cell-specific parameters during cycling, the specific stored energy and the storage temperature were depicted in a calendar ENPOLITE-Plot.

"Table of Contents" TOC Graphic:

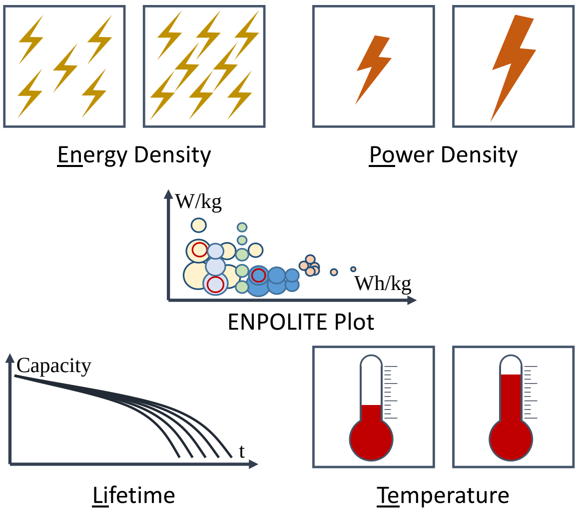

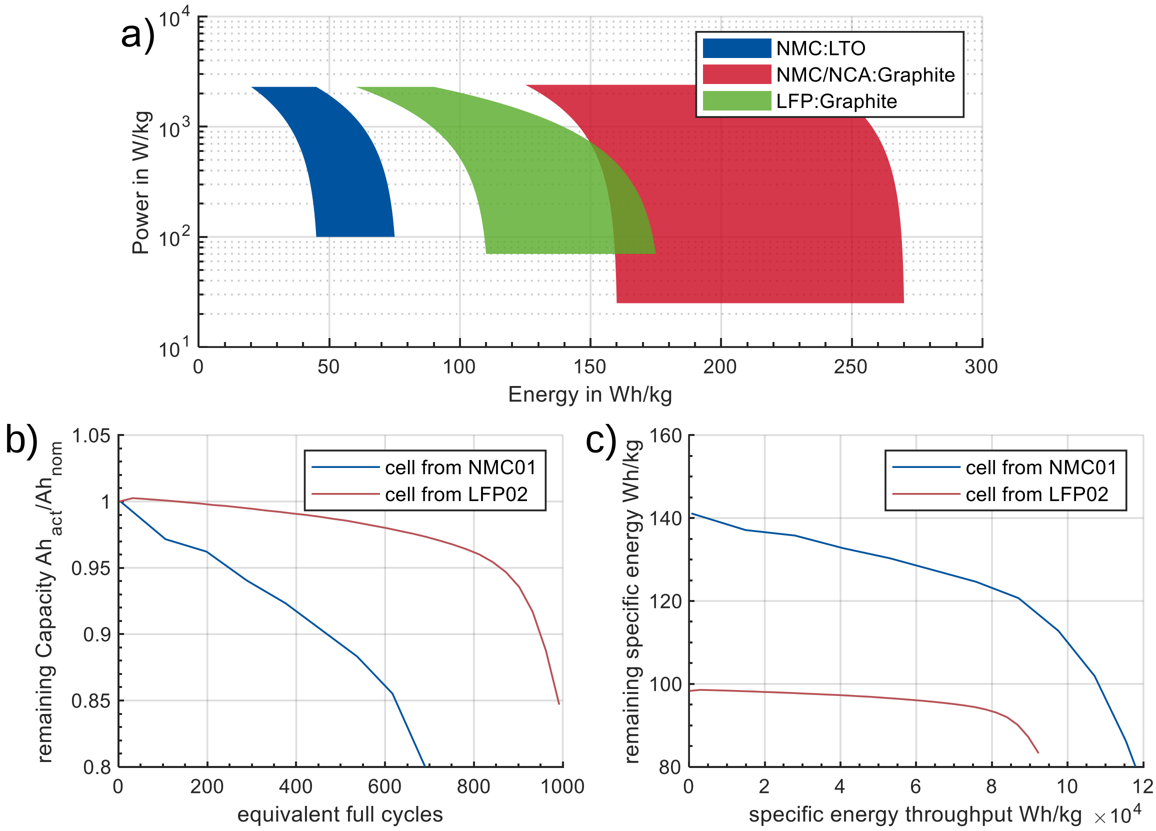

Figure 1: Limitation of existing graphical comparisons of batteries. (a) Ragone plot of different lithium-ion battery chemistries. The plot contains no information about lifetime or different usage scenarios. Cells with a high power density can also be used at a lower power level than depicted. (b), (c) Lifetime comparison of two cells, one from dataset NMC01 and one from dataset LFP02. (b) shows relative capacity vs. equivalent full cycles, while (c) shows remaining specific energy vs. specific energy throughput. Both comparisons are common, but by including weight and energy in the comparison, different conclusions are drawn about the relative lifetime of the cells.

Due to their impressive energy density, power density, lifetime, and cost, lithium-ion batteries have become the most important electrochemical storage system, with applications including consumer electronics, electric vehicles, and stationary energy storage[1]. However, each application has unique, often conflicting product specifications, requiring a balanced overall assessment. The Ragone plot[2], shown in Figure 1a for lithium-ion battery chemistries, is a commonly-used plot to compare two of these specifications, energy and power; however, important parameters including cost, lifetime, and temperature sensitivity are not considered. A standardized and balanced reporting and visualization of specifications would greatly help an informed cell selection process.

Comparisons of energy and power density can be made relatively easily via standard test protocols and within a short timeframe. However, comparing cells across other dimensions presents some practical challenges, particularly in an academic setting. First, even though the price is an essential criterion in many applications, it is also the most controversial since individual cell prices are not openly shared and depend on nontechnical factors such as production volume and operating margin. Second, lifetime comparisons of lithium-ion batteries are widely discussed in the literature[3–8], but these comparisons are especially challenging due to the high sensitivity of lithium-ion battery lifetime to usage conditions (e.g., fast charge, temperature control, cell interconnection, etc.). Additionally, the metrics for lifetime are not standardized, and conclusions about lifetime performance are generally dependent on the choice of metrics used (e.g., relative vs. absolute capacity or energy; see Figures 1b–1c). Furthermore, battery degradation is often nonlinear[8–10]; therefore, using a single parameter from a linear fit (e.g., the slope) to represent nonlinear aging trends must be handled with care. Despite these challenges, standardized reporting and visualization of these parameters is still useful for both fundamental understanding and practical concerns such as cell selection. To this end, bubble plots have been used on the material level to compare lithium metal electrodes on four dimensions[11].

In this work, we introduce ENPOLITE (energy-power-lifetime-temperature) plots to compare cells across various chemistries, designs, and usage conditions. ENPOLITE plots represent multidimensional bubble plots derived from a non-logarithmic version of the Ragone diagram[2]. Leveraging the increasing number of open-source battery datasets, ENPOLITE compares several hundred battery cells within a single bubble plot derived from a raw data set exceeding 1000 GB. While this plot makes some simplifications to represent the multidimensional dataset, it can be effectively used for cell comparison and selection. ENPOLITE plots of aging-related parameters illustrate differences between lifetimes. Although various age-specific variables and metadata are contained in each set of aging data, composed of a dataset of cells, the ENPOLITE plots present a simple two-dimensional graph, allowing easy comparison of individual battery cell types. The Supporting Information depicts an overview of the cells evaluated in this study; we also created a public website (enpolite.org) that hosts interactive versions of these plots.

In contrast to the Ragone plot, the ENPOLITE plots do not show the power and energy capabilities of a cell, but the energy and power density at the respective lifetime's operating condition. Therefore, the same cell type is shown at different energy and power levels when cycling currents or cycle depths are different. The x-axis represents the used specific energy density of the individual battery cell at the beginning of life (BOL) within its aging test and is calculated using Equation 1. In this work, we base calculations on battery cell weight, which is less controversial yet equally important in many technical applications; cell volume-based calculations were also performed and can be found in the Supporting Information.

$$(1)\quad \frac{\Delta \boldsymbol{DOD} \,*\, \boldsymbol{C}_{\mathbf{Cell(BOL)}} \,*\, \overline{\boldsymbol{U}}_{\mathbf{Cycle}}}{\boldsymbol{m}_{\mathbf{Cell}}} = \frac{\mathbf{Wh_{Cycle}}}{\mathbf{kg}}$$

Here, $\Delta\mathbf{DOD}$ represents the cycling depth, $\mathbf{C}_{\mathbf{Cell(BOL)}}$ the discharge capacity, $\overline{\mathbf{U}}_{\mathbf{Cycle}}$ the mean voltage while cycling, and $\mathbf{m}_{\mathbf{Cell}}$ the cell mass. Thus, the x-axis represents the average amount of energy a cell has charged and discharged per kg and per cycle in the completed aging test and describes the battery cell-specific operating point.

The y-axis represents the specific power of the individual battery cells during cycling and is calculated using Equation 2:

$$(2)\ \frac{\overline{\boldsymbol{I}}_{\mathbf{Charge}} * \overline{\boldsymbol{U}}_{\mathbf{Cycle}}}{\boldsymbol{m}_{\mathbf{Cell}}} = \frac{\mathbf{W}_{\mathbf{Charge}}}{\mathbf{kg}}$$

Here, $\overline{\boldsymbol{I}}_{\mathbf{Charge}}$ represents the mean charge current, $\overline{\mathbf{U}}_{\mathbf{Cycle}}$ the mean cycling voltage, and $\mathbf{m}_{\mathbf{Cell}}$ the cell mass. A typical Ragone plot depicts the dischargeable power, which can be used to determine the capability of a cell to fulfill an application requirement. Since charge currents generally have a more significant influence on aging than discharge currents[5,12,13], the y-axis shows the power used while charging. Similar to the x-axis, the y-axis in the ENPOLITE plots is normalized to the cell weights.

The achieved lifetime of the individual cells is also portrayed in the ENPOLITE plots. The comparison of lifetime data requires a measure of aging that normalizes cell weight or volume and reflects the cell realistic usability. It is expressed in the graphic as the bubble area. In this work, the used lifetime coefficient is a linear aging model, expressed in energy throughput per percentage point of cell capacity lost, normalized to the respective cell weight. While the linear model is a simplified description of cell degradation, unable to accurately follow nonlinear aging patterns, it allows a comparison with only one value. Other more complex aging models could be part of further Big-Data lithium-ion aging analysis that can be executed with the datasets used in this paper.

The lifetime coefficient (and therefore the area of the bubble) is calculated using Equation 3:

$$(\mathbf{3})\ \frac{\boldsymbol{N}_{\mathbf{FCE(EOT|EOL)}} * \boldsymbol{C}_{\mathbf{Cell(BOL)}} * \overline{\boldsymbol{U}}_{\mathbf{Cycle}}}{\boldsymbol{m}_{\mathbf{Cell}} * \ \%_{\mathbf{Cap.Loss(EOT|EOL)}}} = \frac{\mathbf{Wh}_{\mathbf{Throughput}}}{\mathbf{kg}\ * \%_{\mathbf{Cap.Loss}}}$$

Here, $N_{\mathrm{FCE(EOT|EOL)}}$ represents the equivalent full cycles to reach the end-of-life-criterion (EOL) or the end of the test (EOT), $\mathbf{C}_{\mathbf{Cell(BOL)}}$ the discharge capacity, $\overline{\mathbf{U}}_{\mathbf{Cycle}}$ the mean cycling voltage, $\mathbf{m}_{\mathbf{Cell}}$ the cell mass, and $\%_{\mathrm{Cap.Loss(EOT|EOL)}}$ the capacity percentage points lost. If raw data is available, the charge throughput is extracted directly. A doubling of the circle area is equivalent to a doubling of the lifetime coefficient.

In line with published literature, the lifetime linearization was normalized to a relative capacity loss of 20%. If cells did not lose 20% of their initial capacity within their aging tests, the linearization was based on their EOT. Generally, different EOL criteria can also be used. Unlike most published lifetime comparisons, the lifetime coefficient calculated here also considers cell size and compares battery cells using the mass-normalized energy throughput. Thus, different cell masses, charge throughputs, and cycling voltages, driven by different mean DODs and different cell chemistries, can be considered.

Finally, the cell-specific cycling temperature also plays a decisive role in explaining the aging behavior of lithium-ion cells[5]. The color of each bubble circumference depicts the cell temperature during cycling, providing vital information to explain differences in individual cell lifetimes at similar operation points. If available, the mean cycling temperature at the can or pouch of the cell is used. If the individual cell temperature is not available, the temperature chamber setpoint was used. It should be noted that the temperature within a cell and within the temperature chamber can vary significantly, especially for high power cycling. For cells without extractable cycling temperature, the bubble circumference is grey.

With the values for the x- and y-axis and the lifetime bubble area established, all cyclic aging datasets can be sorted into the ENPOLITE plot. Figure 2 (a) shows the translation of an initial aging test result to the ENPOLITE plot for a cell from a data set with 2.9 Ah LTO cells. In addition to the metadata (cell chemistry, nominal capacity, cell format, cycling time) of the individual datasets, Figure 2b depicts an ENPOLITE plot of one complete data set of 10 cells. Not surprisingly, we find that cells cycled at higher temperatures (i.e., red-colored bubble edges) also have shorter lifetimes (i.e., bubble sizes).

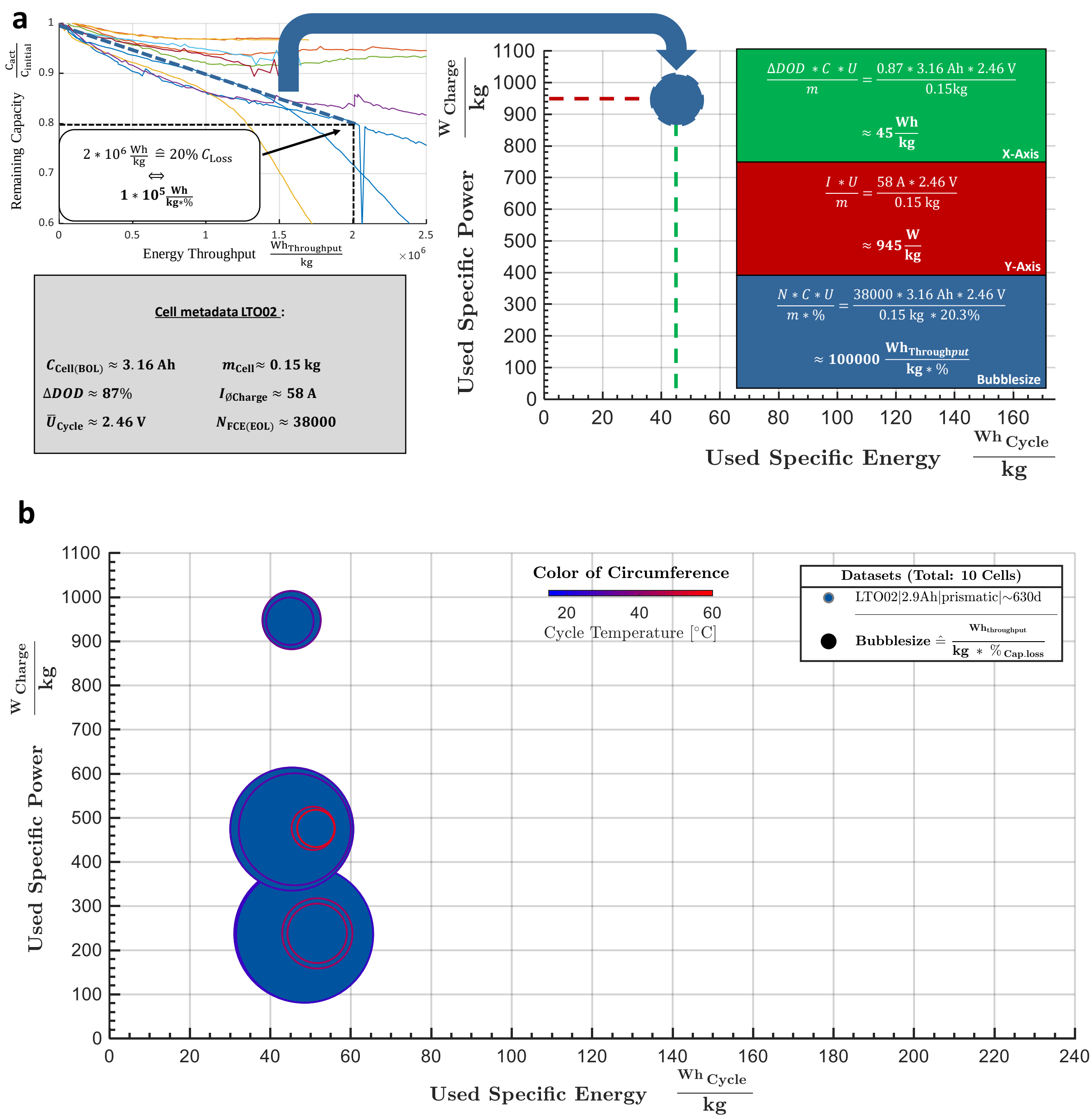

Figure 2: (a) Calculation of a single bubble data point for the ENPOLITE plot. Data for one individual cell from dataset LTO02 was added in the cyclic lifetime diagram; relevant metadata for the lifetime coefficient calculations are given in the lower-left corner. The

green area shows the calculation for the x-axis; the red area shows the calculation for the y-axis; the blue color shows the calculation for the lifetime coefficient and is reflected in the bubble area within the graphic. A higher lifetime coefficient and more normalized energy throughput are reflected in a larger bubble area.

(b) Dataset LTO02 with 10 cells illustrated in the ENPOLITE plot; the color of the bubble circumference, which corresponds to the temperature, explains the differences in the lifetime coefficient for cells with similar electric operating points.

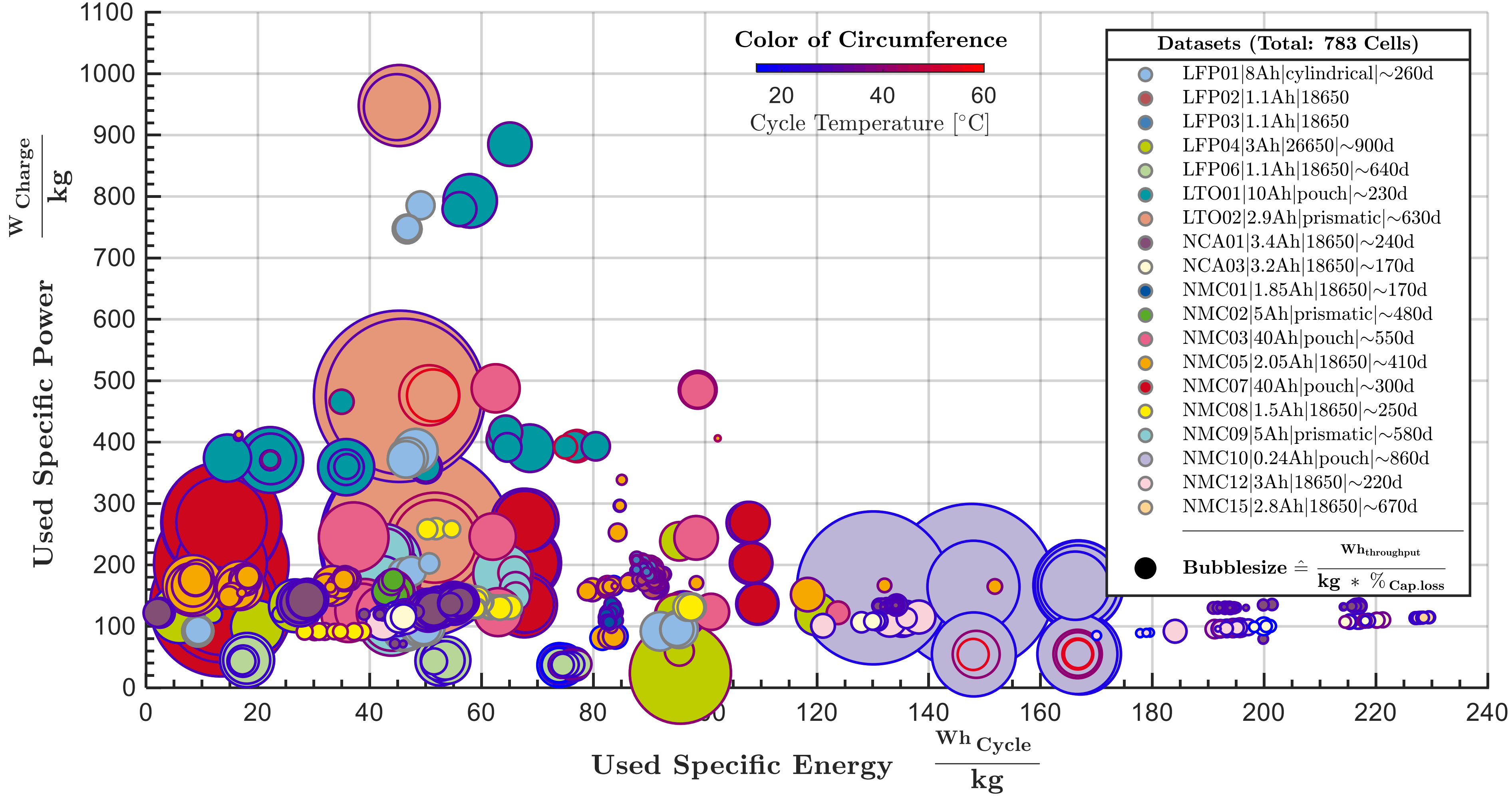

Figure 3: Complete cyclic ENPOLITE lifetime plot with 783 cells. An interactive version can be found online at enpolite.org

Figure 3 shows the complete ENPOLITE plot for the cyclic aging tests of 783 different cells from 19 datasets. An interactive version and detailed description can be found in the Supporting Information and on the website (enpolite.org). In total, the ENPOLITE plot in Figure 3 displays eight critical parameters determining the lifetime behavior of lithium-ion battery cells: i) used energy density, ii) used power density, and iii) energy throughput per percentage point, as well as the metadata on the aging test including iv) cycle temperature, v) cycle duration, vi) cell chemistry, vii) cell format, and viii) nominal capacity. The plot reflects the general trend that lifetimes tend to decrease with higher energy densities and power densities. The dark-yellow-colored dataset with cells from Devie et al.[14] (NMC15|2.8Ah|18650|~670d.) shows the highest used specific energy with up to 230 Wh/kg. The high energy cells from LG Chem were cycled at 100% DOD. Only a few cells achieved above-average lifetimes at either high energy or high power densities, such as the dark-blue-colored dataset (NMC10|0.24Ah|pouch|~860d.) from Harlow et al.[15]. Furthermore, we also observe that high power densities were only achieved in conjunction with lower energy densities. In most datasets, higher cycling temperatures resulted in a reduced lifetime, corroborating the well-known behavior of lithium-ion battery cells. This can also be seen for the above mentioned NMC10 cells at 165 Wh/kg and 50 W/kg, for which the circle area significantly decreases for cells cycled at higher temperatures within the same operating point. Occasionally, tiny data points are also visible, representing cells quickly destroyed at their operating point in the aging test, for example, due to lithium plating at low temperatures. The exceptionally high lifetimes of cells with Lithium Titanate (LTO) anodes are also well represented; the peach-colored dataset (LTO02|2.9Ah|prismatic|~630d.) of Nemeth and Schröer et al.[16,17] stands out with the highest lifetime observed of any cells in this plot. Furthermore, these cells also achieve the highest used specific power with up to 950 W/kg, which corresponds to current rates of up to 20C. Lastly, neighboring data points with a similar circumference color but strongly differing circle areas illustrate cell-to-cell aging variation within a dataset, with an in-depth evaluation in an upcoming paper.

We also created an ENPOLITE plot depicting calendar life using a similar approach. The X-axis for the calendar ENPOLITE plot depicts the state of charge (SOC) of the cells in storage; we express this as the usable stored energy in the cell normalized to its weight. The used specific storage energy coefficient was calculated using Equation 4:

$$(4)\ \frac{\boldsymbol{C}_{\mathbf{Cell(BOL)}} * \boldsymbol{U}_{\mathbf{nom}} * \boldsymbol{SOC}_{\mathbf{Storage}}}{\boldsymbol{m}_{\mathbf{Cell}}} = \frac{\mathbf{Wh_{SOC}}}{\mathbf{kg}}$$

Here, $\mathbf{C}_{\mathbf{Cell(BOL)}}$ represents the discharge capacity at beginning of life, $\boldsymbol{U}_{\mathbf{nom}}$ the nominal voltage, $\boldsymbol{SOC}_{\mathbf{Storage}}$ the state of charge, and $\mathbf{m}_{\mathbf{Cell}}$ the cell mass.

The X-axis indicates how much energy per kg was stored by the cell at the beginning of life (BOL), and the Y-axis coefficient represents the cell storage temperature in degrees Celsius (°C).

Figure 4 depicts a calendar ENPOLITE diagram, representing 307 calendar-aged cells in total. In this plot, the typical calendar aging test matrices are readily recognized. Most cells are stored at temperatures of 25°C, 40 °C, or 50 °C. Each cell type is typically stored at multiple SOC levels; therefore, multiple points of the used specific storage energy are shown.

Similar to the cyclic ENPOLITE plot, an aging measure was developed for the calendar aging data, which better reflects the battery cells' actual usability than the relative loss of capacity metric often used in literature. The passive anode effect[18,19], commonly seen in calendar tests, was included in the evaluation and described in detail in the Supporting Information. The aging coefficient's bubble area corresponds to the number of days until the cell energy density is reduced by 1 Wh/kg due to degrading capacity. The lifetime coefficient was calculated using Equation 5:

$$(5)\ \frac{\boldsymbol{Date}_{\mathbf{T2}} - \boldsymbol{Date}_{\mathbf{T1}}}{\frac{(\boldsymbol{C}_{\mathbf{T1}} - \boldsymbol{C}_{\mathbf{T2}}) * \boldsymbol{U}_{\mathbf{nom}}}{\boldsymbol{m}_{\mathbf{Cell}}}} = \frac{\mathbf{Days}}{\frac{\mathbf{Wh_{Lost}}}{\mathbf{kg}}}$$

Here, $\boldsymbol{Date}_{\mathbf{T2}} - \boldsymbol{Date}_{\mathbf{T1}}$ represents the time difference between measurements, $\boldsymbol{C}_{\mathbf{T1}}$ and $\boldsymbol{C}_{\mathbf{T2}}$ the first and second capacity measurements, $(C_{\mathrm{T1}} - C_{\mathrm{T2}})$ the capacity lost between measurements, $\boldsymbol{U}_{\mathbf{nom}}$ the nominal voltage, and $\mathbf{m_{Cell}}$ the cell mass.

The structure and input of each data point with respect to the X- and Y-axis and the size of the circle area, represented by the aging coefficient, are similar to the cyclic diagram structure shown in Figure 2. For the representation of the calendar lifetime data, however, some striking differences have to be considered.

Particularly in calendar aging tests, cells sometimes retain over 100% of their initial capacity even after a long aging period. Examples of this can be found in dataset NMC11 from Harlow et al.[15] It can be seen that individual cells still increase in capacity even up to the last capacity measurement published after 580 days. However, an increase in capacity in the linear part of the aging process leads to a negative value by definition of the used lifetime coefficient according to the formula above. For this reason, the value ∞ was inserted into the calendar ENPOLITE plot. This value does not imply that the cells last forever but is used when the lifetime coefficient cannot be evaluated because the corresponding cell capacities are still rising. The size of these bubbles is fixed and does not represent an absolute lifetime; they should not be compared with other datapoint sizes. Cell data with this exception are illustrated with transparent shading in the calendar ENPOLITE plot and may in fact point to excellent durability.

Figure 4 shows the ENPOLITE plot of calendar lifetime data for a total of 307 cells from 11 datasets. A reference bubble, equivalent to 100 days to a loss of 1 Wh/kg, can be found in the bottom-right corner of the diagram for better estimation of the bubble area. In this diagram, a doubling of the circle area also doubles the calculated lifetime coefficient.

Generally, Figure 4 illustrates that cells stored at higher energy/charge states lose storable energy (and thus capacity) faster than cells stored at low energy/charge states. Used specific storage energies range from 0 Wh/kg (0% SOC) up to 225 Wh/kg represented by the dark-red-colored dataset (NCA04|2.8Ah|18650|~290d.) from Keil et al.[20], which were stored at 100% SOC at 25 °C and 50 °C, respectively. Outstanding lifetimes were achieved by lithium-nickel-manganese-cobalt-oxide (NMC) cells (NMC11|0.24Ah|pouch|~580d.) from Harlow et al.[15], depicted by turquoise dots, even at high used specific storage energies. Especially at 20 °C, they outperformed other cells without visible aging after 580 days even at high SOC. The authors attributed this to the single-crystal structure of the NMC532 cathode particles and electrolyte additives[15]. The influence of the storage temperatures on the lifetimes is also clearly visible. In general, within all datasets, higher temperatures were associated with shortened lifetime. Few data points were aged below 20 °C and none of these belonged to the datasets showing the longest lifetime. No cells tested above 60 °C were part of the datasets in the calendar ENPOLITE plot, since side reactions prevent valid accelerated aging tests[21].

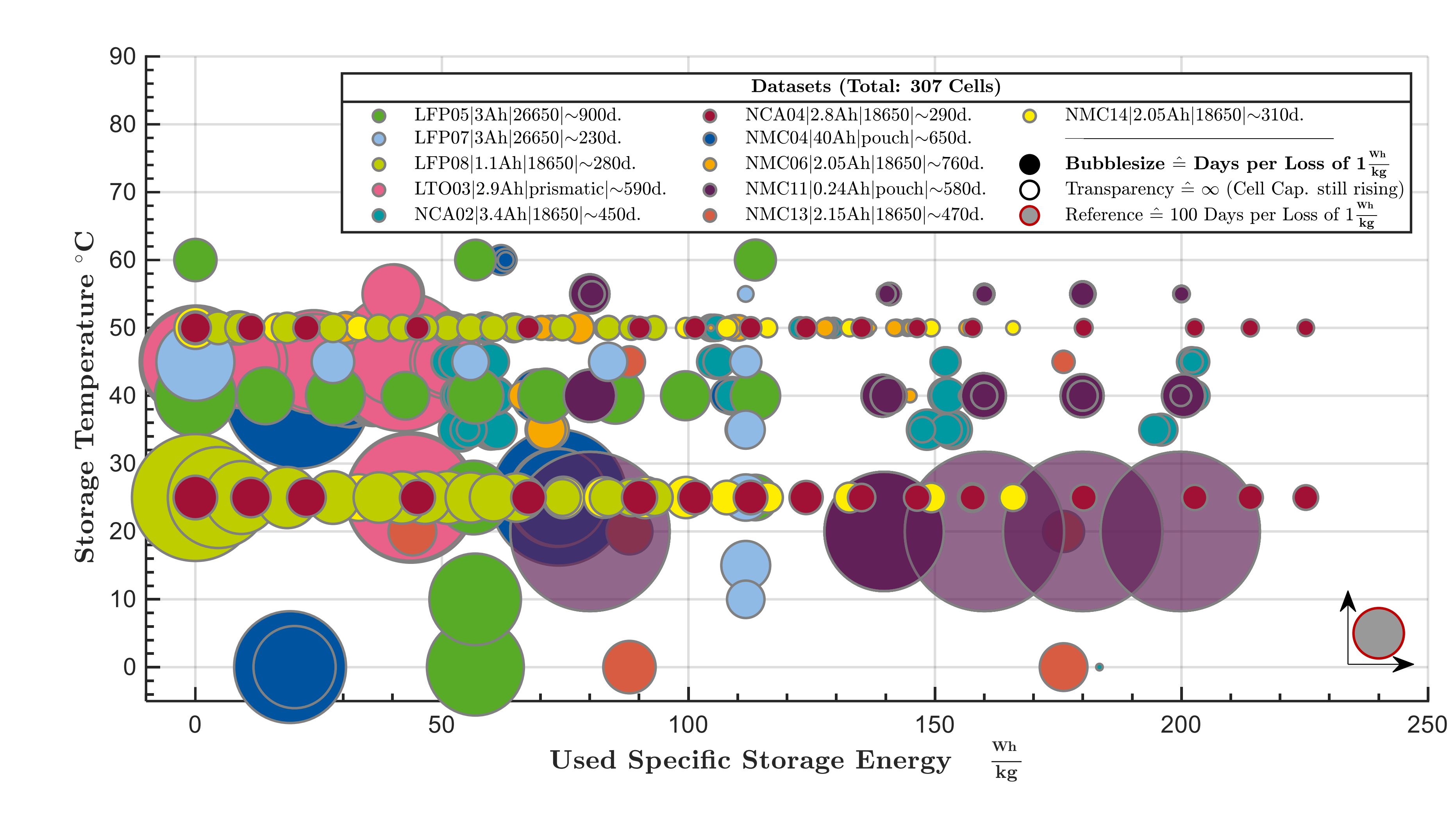

Figure 4: Complete calendar ENPOLITE lifetime plot with 307 cells. An interactive version of the plot can be found online at enpolite.org

Conclusion:

Lithium-ion batteries must satisfy multiple requirements for a given application, including energy density, power density, and lifetime. However, visualizing the tradeoffs between these requirements is often challenging; for instance, battery aging data is presented as a line plot with capacity fade versus cycle count, a difficult format for viewing multiple datasets. Also, standard lifetime plots can be challenging to interpret (e.g., high cycle count with low energy throughput). In this work, we introduced the ENPOLITE plots, which can be used to compare large datasets of lithium-ion battery cycling and calendar aging across multiple battery chemistries and usage conditions. ENPOLITE plots capture performance metrics that are relevant for applications. Similar comprehensive representations of large datasets of variable battery aging data were, to the best of our knowledge, never before shown in published literature. ENPOLITE plots (and, more generally, multidimensional plotting) may greatly facilitate informed decisions on battery technology development. Some of the observations were known before, e.g., that LTO are suitable for high power, or that batteries cannot be both high power and high energy density. This commonplace knowledge is now substantiated by specific values for energy and power application-specific selection. The ENPOLITE plots also reveal exemplary cells across a number of dimensions. As the battery community continues to publish data, particularly on new chemistries, the ENPOLITE plots enable unbiased comparisons of key operating parameters to be added to published battery databases. Finally, we mention that with non-uniform data formats being the biggest hurdle for inclusion of additional datasets, the battery community would greatly benefit from standardized and uniform battery data formats for automated evaluation.

Appendix:

Table I. Summary of all datasets used in this work.

Cell type identifier	Identifier	Raw data/ External	#	Brief description: Cell name, nominal capacity, format	Aging-Type	Test-duration	Ref, Year
e-production	NMC01	Raw data	48	Sanyo UR18650E, 1.85 Ah, 18650	Cyc.	~170d	[22], 2014
	NMC02	Raw data	24	Sanyo UF121285, 5 Ah, prismatic	Cyc.	~480d	
GOELK	NMC03	Raw data	13	LiTec 40 Ah, pouch	Cyc.	~550d	[23], 2019
	NMC04	Raw data	30	LiTec 40 Ah, pouch	Cal.	~650d	[23], 2019
FutureBus	LTO01	Raw data	23	Microvast 10 Ah, pouch	Cyc.	~230d	[24], 2019
e-performance	NMC05	Raw data	65	Sanyo UR18650E, 2.05 Ah, 18650	Cyc.	~410d	[25], 2014
	NMC06	Raw data	48	Sanyo UR18650E, 2.05 Ah, 18650	Cal.	~450d	[26], 2014
HV-Modal	LTO02	Raw data	10	Toshiba SCiB 2.9 Ah, prismatic	Cyc.	~630d	[16,17], 2020
	LTO03	Raw data	16	Toshiba SCiB 2.9 Ah, prismatic	Cal.	~590d	[16,17], 2020
MobilEM	NCA01	Raw data	183	Samsung INR18650-35E, 3.4 Ah, 18650	Cyc.	~240d	[27], 2020
	NCA02	Raw data	60	Samsung INR18650-35E, 3.4 Ah, 18650	Cal.	~450d	
LiMobility	NMC07	Raw data	27	440-Kokam, 40 Ah, pouch	Cyc.	~300d	[28], 2015
HiEnd	LFP01	Raw data	26	OMLIFE8AHC-HP, 8 Ah, cylindrical	Cyc.	~260d	[29], 2016
DriveBattery	NMC08	Raw data	39	Samsung INR18650-15L, 1.5 Ah, 18650	Cyc.	~250d	[30], 2017
	NMC09	Raw data	27	Hitachi 5 Ah, prismatic	Cyc.	~580d	[30], 2017

Severson et al.	LFP02	Raw data	124	A123 APR18650M1A, 1.1 Ah, 18650	Cyc.	-	[9], 2019
Attia et al.	LFP03	Raw data	45	A123 APR18650M1A, 1.1 Ah, 18650	Cyc.	-	[31],2020
Naumann et al. &	LFP04	External	14	Sony US26650FTC1, 3 Ah, 26650	Cyc.	~900d	[32,33], 2020
Spingler et al.	LFP05	External	17	Sony US26650FTC1, 3 Ah, 26650	Cal.	~900d	[34], 2020
Harlow et al.	NMC10	External	11	Li-FUN Technology 0.24 Ah, pouch	Cyc.	~860d	[15], 2019
	NMC11	External	24	Li-FUN Technology 0.24 Ah, pouch	Cal.	~580d	[15], 2019
Preger et al.	LFP06	Raw data	28	A123 APR18650M1A, 1.1 Ah, 18650	Cyc.	~640d	[8], 2020
	NCA03	Raw data	22	Panasonic NCR18650B, 3.2 Ah, 18650	Cyc.	~170d	[8], 2020
	NMC12	Raw data	24	LG Chem 18650HG2, 3 Ah, 18650	Cyc.	~220d	[8], 2020
Schmitt et al.	NMC13	External	8	Sony US18650V3, 2.15 Ah, 18650	Cal.	~470d	[35], 2017
Schimpe et al.	LFP07	External	10	Sony US26650FTC1, 3 Ah, 26650	Cal.	~230d	[36], 2018
Keil et al.	NMC14	External	32	Sanyo UR18650E, 2.05 Ah, 18650	Cal.	~310d	[37], 2016
	LFP08	External	32	A12318650M1A, 1.1 Ah, 18650	Cal.	~280d	[37], 2016
	NCA04	External	32	Panasonic NCR18650PD, 2.8 Ah, 18650	Cal.	~290d	[20], 2016
Devie et al.	NMC15	Raw data	15	LG Chem ICR18650C2, 2.8 Ah, 18650	Cyc.	~670d	[14], 2018

Acronyms

BOL	beginning of life
DOD	depth of discharge / cycling depth
EOL	end of life
EOT	end of test
FCE	full cycle equivalent
LFP	lithium iron phosphate (Cathode material)
LTO	lithium titanate (Anode material)
NCA	lithium nickel cobalt aluminum oxide (Cathode material)
NMC	lithium nickel manganese cobalt oxide (Cathode material)

Additional acronyms can be found in the supporting Information

Acknowledgments: This work was mainly supported by the German Federal Ministry for Economic Affairs and Energy (BMWi) within the research project "E2Fuels" (03EIV011F) and "Topologieanalyse von Speichersystemen" (IGF 18957 N/1). Y.P. was supported by the U.S. Department of Energy, Office of Electricity, Energy Storage Program. Sandia National Laboratories is a multi-mission laboratory managed and operated by The National Technology & Engineering Solutions of Sandia, LLC, which is a wholly owned subsidiary of Honeywell International Inc., for the U.S. Department of Energy's National Nuclear Security Administration under contract DE-NA0003525. This paper describes objective technical results and analysis. Any subjective views or opinions that might be expressed in the paper do not necessarily represent the views of the U.S. Department of Energy or the United States Government. The authors would like to thank J. Harlow and J. Dahn from Dalhousie University for providing updated data on their publication. P.D. thanks P. Althoff for support on the interactive version of the plot and website. The authors also thank V. De Angelis for his insights. The raw data for references [8] and [14] was downloaded from www.batteryarchive.org.

Supporting Information Available: Calculations are shown in detail, datasets are shown in more detail, and an interactive version of the ENPOLITE plots can be found on www.enpolite.org.

ORCID:
Philipp Dechent: 0000-0003-3041-1436
Alexander Epp: 0000-0002-6202-0213
Dominik Jöst: 0000-0002-5731-5666
Yuliya Preger: 0000-0001-8558-2529
Peter M. Attia: 0000-0003-4745-5726
Weihan Li: 0000-0002-2916-3968
Dirk Uwe Sauer: 0000-0002-5622-3591

Author contribution: P.D., D.J., Conceptualization and Methodology. P.D., A.E., D.J., W.L. created the software for data analysis. Y.P. and P.M.A. provided valuable advice and guidance for preparing the analysis and interpreting the results. P.D., D.J., and D.U.S provided funding acquisition. P.D. and A.E. wrote the original draft. All authors worked on Writing - Review & Editing

References

(1) Figgener, J.; Stenzel, P.; Kairies, K.-P.; Linßen, J.; Haberschusz, D.; Wessels, O.; Angenendt, G.; Robinius, M.; Stolten, D.; Sauer, D. U. The Development of Stationary Battery Storage Systems in Germany – A Market Review. *Journal of Energy Storage* **2020**, *29*, 101153. https://doi.org/10.1016/j.est.2019.101153.

(2) Ragone, D. V. Review of Battery Systems for Electrically Powered Vehicles; 1968; p 680453. https://doi.org/10.4271/680453.

(3) Sikha, G.; Ramadass, P.; Haran, B. S.; White, R. E.; Popov, B. N. Comparison of the Capacity Fade of Sony US 18650 Cells Charged with Different Protocols. *Journal of Power Sources* **2003**, *122* (1), 67–76. https://doi.org/10.1016/S0378-7753(03)00027-2.

(4) Käbitz, S.; Gerschler, J. B.; Ecker, M.; Yurdagel, Y.; Emmermacher, B.; Andri, D.; Mitsch, T.; Sauer, D. U. Cycle and Calendar Life Study of a Graphite|LiNi1/3Mn1/3Co1/3O2 Li-Ion High Energy System. Part A: Full Cell Characterization. *Journal of Power Sources* **2013**, *239*, 572–583. https://doi.org/10.1016/j.jpowsour.2013.03.045.

(5) Ecker, M.; Gerschler, J. B.; Vogel, J.; Käbitz, S.; Hust, F.; Dechent, P.; Sauer, D. U. Development of a Lifetime Prediction Model for Lithium-Ion Batteries Based on Extended Accelerated Aging Test Data. *Journal of Power Sources* **2012**, *215*, 248–257. https://doi.org/10.1016/j.jpowsour.2012.05.012.

(6) Dubarry, M.; Truchot, C.; Liaw, B. Y. Cell Degradation in Commercial LiFePO4 Cells with High-Power and High-Energy Designs. *Journal of Power Sources* **2014**, *258*, 408–419. https://doi.org/10.1016/j.jpowsour.2014.02.052.

(7) Dubarry, M.; Qin, N.; Brooker, P. Calendar Aging of Commercial Li-Ion Cells of Different Chemistries – A Review. *Current Opinion in Electrochemistry* **2018**. https://doi.org/10.1016/j.coelec.2018.05.023.

(8) Preger, Y.; Barkholtz, H. M.; Fresquez, A.; Campbell, D. L.; Juba, B. W.; Romàn-Kustas, J.; Ferreira, S. R.; Chalamala, B. R. Degradation of Commercial Lithium-Ion Cells as a Function of Chemistry and Cycling Conditions. *J. Electrochem. Soc.* **2020**. https://doi.org/10.1149/1945-7111/abae37.

(9) Severson, K. A.; Attia, P. M.; Jin, N.; Perkins, N.; Jiang, B.; Yang, Z.; Chen, M. H.; Aykol, M.; Herring, P. K.; Fraggedakis, D.; Bazant, M. Z.; Harris, S. J.; Chueh, W. C.; Braatz, R. D. Data-Driven Prediction of Battery Cycle Life before Capacity Degradation. *Nature Energy* **2019**, *4* (5), 383–391. https://doi.org/10.1038/s41560-019-0356-8.

(10) Dubarry, M.; Baure, G.; Devie, A. Durability and Reliability of EV Batteries under Electric Utility Grid Operations: Path Dependence of Battery Degradation. *J. Electrochem. Soc.* **2018**, *165* (5), A773–A783. https://doi.org/10.1149/2.0421805jes.

(11) Albertus, P.; Babinec, S.; Litzelman, S.; Newman, A. Status and Challenges in Enabling the Lithium Metal Electrode for High-Energy and Low-Cost Rechargeable Batteries. *Nature Energy* **2018**, *3* (1), 16–21. https://doi.org/10.1038/s41560-017-0047-2.

(12) Wu, Y.; Keil, P.; Schuster, S. F.; Jossen, A. Impact of Temperature and Discharge Rate on the Aging of a LiCoO2/LiNi0.8Co0.15Al0.05O2 Lithium-Ion Pouch Cell. *J. Electrochem. Soc.* **2017**, *164* (7), A1438–A1445. https://doi.org/10.1149/2.0401707jes.

(13) Anseán, D.; Dubarry, M.; Devie, A.; Liaw, B. Y.; García, V. M.; Viera, J. C.; González, M. Fast Charging Technique for High Power LiFePO4 Batteries: A Mechanistic Analysis of Aging. *Journal of Power Sources* **2016**, *321*, 201–209. https://doi.org/10.1016/j.jpowsour.2016.04.140.

(14) Devie, A.; Baure, G.; Dubarry, M. Intrinsic Variability in the Degradation of a Batch of Commercial 18650 Lithium-Ion Cells. *Energies* **2018**, *11* (5), 1031. https://doi.org/10.3390/en11051031.

(15) Harlow, J. E.; Ma, X.; Li, J.; Logan, E.; Liu, Y.; Zhang, N.; Ma, L.; Glazier, S. L.; Cormier, M. M. E.; Genovese, M.; Buteau, S.; Cameron, A.; Stark, J. E.; Dahn, J. R. A Wide Range of Testing Results on an Excellent Lithium-Ion Cell Chemistry to Be Used as Benchmarks for New Battery Technologies. *J. Electrochem. Soc.* **2019**, *166* (13), A3031. https://doi.org/10.1149/2.0981913jes.

(16) Nemeth, T.; Schröer, P.; Kuipers, M.; Sauer, D. U. Lithium Titanate Oxide Battery Cells for High-Power Automotive Applications – Electro-Thermal Properties, Aging Behavior and Cost Considerations. *Journal of Energy Storage* **2020**, *31*, 101656. https://doi.org/10.1016/j.est.2020.101656.

(17) Schröer, P.; Khoshbakht, E.; Nemeth, T.; Kuipers, M.; Zappen, H.; Sauer, D. U. Adaptive Modeling in the Frequency and Time Domain of High-Power Lithium Titanate Oxide Cells in Battery Management Systems. *Journal of Energy Storage* **2020**, *32*, 101966. https://doi.org/10.1016/j.est.2020.101966.

(18) Lewerenz, M.; Fuchs, G.; Becker, L.; Sauer, D. U. Irreversible Calendar Aging and Quantification of the Reversible Capacity Loss Caused by Anode Overhang. *Journal of Energy Storage* **2018**, *18*, 149–159. https://doi.org/10.1016/j.est.2018.04.029.

(19) Zilberman, I.; Sturm, J.; Jossen, A. Reversible Self-Discharge and Calendar Aging of 18650 Nickel-Rich, Silicon-Graphite Lithium-Ion Cells. *Journal of Power Sources* **2019**, *425*, 217–226. https://doi.org/10.1016/j.jpowsour.2019.03.109.

(20) Keil, P.; Jossen, A. Calendar Aging of NCA Lithium-Ion Batteries Investigated by Differential Voltage Analysis and Coulomb Tracking. *J. Electrochem. Soc.* **2016**, *164* (1), A6066. https://doi.org/10.1149/2.0091701jes.

(21) MacNeil, D. D.; Lu, Z.; Chen, Z.; Dahn, J. R. A Comparison of the Electrode/Electrolyte Reaction at Elevated Temperatures for Various Li-Ion Battery Cathodes. *Journal of Power Sources* **2002**, *108* (1), 8–14. https://doi.org/10.1016/S0378-7753(01)01013-8.

(22) Baumhöfer, T.; Brühl, M.; Rothgang, S.; Sauer, D. U. Production Caused Variation in Capacity Aging Trend and Correlation to Initial Cell Performance. *Journal of Power Sources* **2014**, *247*, 332–338. https://doi.org/10.1016/j.jpowsour.2013.08.108.

(23) Schoeneberger, I.; Dechent, P.; Rücker, F.; Jakobowski, S.; Sauer, D. U. Improving Aging Prediction for Electric Vehicle Operation with Combined Electrical, Thermal and Aging Model for Lithium-Ion Battery Packs Using Quantitative Cell Data. *Meet. Abstr.* **2019**, *MA2019-04* (2), 104. https://doi.org/10.1149/MA2019-04/2/104.

(24) Liu, S.; Winter, M.; Lewerenz, M.; Becker, J.; Sauer, D. U.; Ma, Z.; Jiang, J. Analysis of Cyclic Aging Performance of Commercial Li4Ti5O12-Based Batteries at Room Temperature. *Energy* **2019**, *173*, 1041–1053. https://doi.org/10.1016/j.energy.2019.02.150.

(25) Schmalstieg, J.; Käbitz, S.; Ecker, M.; Sauer, D. U. A Holistic Aging Model for Li(NiMnCo)O2 Based 18650 Lithium-Ion Batteries. *Journal of Power Sources* **2014**, *257*, 325–334. https://doi.org/10.1016/j.jpowsour.2014.02.012.

(26) Ecker, M.; Nieto, N.; Käbitz, S.; Schmalstieg, J.; Blanke, H.; Warnecke, A.; Sauer, D. U. Calendar and Cycle Life Study of Li(NiMnCo)O2-Based 18650 Lithium-Ion Batteries. *Journal of Power Sources* **2014**, *248*, 839–851. https://doi.org/10.1016/j.jpowsour.2013.09.143.

(27) Willenberg, L.; Dechent, P.; Fuchs, G.; Teuber, M.; Eckert, M.; Graff, M.; Kürten, N.; Sauer, D. U.; Figgemeier, E. The Development of Jelly Roll Deformation in 18650 Lithium-Ion Batteries at Low State of Charge. *J. Electrochem. Soc.* **2020**, *167* (12), 120502. https://doi.org/10.1149/1945-7111/aba96d.

(28) Marongiu, A.; Roscher, M.; Sauer, D. U. Influence of the Vehicle-to-Grid Strategy on the Aging Behavior of Lithium Battery Electric Vehicles. *Applied Energy* **2015**, *137*, 899–912. https://doi.org/10.1016/j.apenergy.2014.06.063.

(29) Marongiu, A.; Nußbaum, F. G. W.; Waag, W.; Garmendia, M.; Sauer, D. U. Comprehensive Study of the Influence of Aging on the Hysteresis Behavior of a Lithium Iron Phosphate Cathode-Based Lithium Ion Battery – An Experimental Investigation of the Hysteresis. *Applied Energy* **2016**, *171*, 629–645. https://doi.org/10.1016/j.apenergy.2016.02.086.

(30) Lehner, S. *Reliability Assessment of Lithium-Ion Battery Systems with Special Emphasis on Cell Performance Distribution*; Aachener Beiträge des ISEA; Shaker Verlag: Aachen, 2017.

(31) Attia, P. M.; Grover, A.; Jin, N.; Severson, K. A.; Markov, T. M.; Liao, Y.-H.; Chen, M. H.; Cheong, B.; Perkins, N.; Yang, Z.; Herring, P. K.; Aykol, M.; Harris, S. J.; Braatz, R. D.; Ermon, S.; Chueh, W. C. Closed-Loop Optimization of Fast-Charging Protocols for Batteries with Machine Learning. *Nature* **2020**, *578* (7795), 397–402. https://doi.org/10.1038/s41586-020-1994-5.

(32) Naumann, M.; Spingler, F. B.; Jossen, A. Analysis and Modeling of Cycle Aging of a Commercial LiFePO4/Graphite Cell. *Journal of Power Sources* **2020**, *451*, 227666. https://doi.org/10.1016/j.jpowsour.2019.227666.

(33) Spingler, F. B.; Naumann, M.; Jossen, A. Capacity Recovery Effect in Commercial LiFePO4 / Graphite Cells. *J. Electrochem. Soc.* **2020**, *167* (4), 040526. https://doi.org/10.1149/1945-7111/ab7900.

(34) Naumann, M.; Schimpe, M.; Keil, P.; Hesse, H. C.; Jossen, A. Analysis and Modeling of Calendar Aging of a Commercial LiFePO4/Graphite Cell. *Journal of Energy Storage* **2018**, *17*, 153–169. https://doi.org/10.1016/j.est.2018.01.019.

(35) Schmitt, J.; Maheshwari, A.; Heck, M.; Lux, S.; Vetter, M. Impedance Change and Capacity Fade of Lithium Nickel Manganese Cobalt Oxide-Based Batteries during Calendar Aging. *Journal of Power Sources* **2017**, *353*, 183–194. https://doi.org/10.1016/j.jpowsour.2017.03.090.

(36) Schimpe, M.; Kuepach, M. E. von; Naumann, M.; Hesse, H. C.; Smith, K.; Jossen, A. Comprehensive Modeling of Temperature-Dependent Degradation Mechanisms in Lithium Iron Phosphate Batteries. *J. Electrochem. Soc.* **2018**, *165* (2), A181. https://doi.org/10.1149/2.1181714jes.

(37) Keil, P.; Schuster, S.; Wilhelm, J.; Travi, J.; Hauser, A.; Karl, R.; Jossen, A. Calendar Aging of Lithium-Ion Batteries: I. Impact of the Graphite Anode on Capacity Fade. *Journal of The Electrochemical Society* **2016**, *163*, A1872–A1880. https://doi.org/10.1149/2.0411609jes.

Supplementary Material:

Table of contents

An in-depth explanation for the ENPOLITE Plot:

The ENPOLITE-Diagram combines four elementary cell parameters of lithium-ion battery aging tests:

Energy, **Po**wer, **Li**fetime, **Te**mperature

Due to its structure, the ENPOLITE-Diagram enables lifetime comparisons among different aging tests while simultaneously illustrating the cell operating points. It enables an application-oriented comparison to be carried out about the aging parameters for a large number of different cells.

Acronyms

BOL	beginning of life
DOD	depth of discharge
EOL	end of life
EOT	end of test
FCE	full cycle equivalent
LFP	lithium iron phosphate (Cathode material)
LTO	lithium titanate (Anode material)
NCA	lithium nickel cobalt aluminum oxide (Cathode material)
NMC	lithium nickel manganese cobalt oxide (Cathode material)

Cell parameter table: Brief explanation

Size	Explanation of evaluation
$\boldsymbol{C}_{\mathbf{Cell(BOL)}}$	For datasets with raw data, this is the first extractable full discharge capacity for every individual cell. For external datasets, the first measured capacity, which was sometimes the charge and sometimes the discharge capacity, was extracted. Often this was the 1C discharge capacity. For external datasets which only had an aging chart, the cell nominal capacity was used.
$\boldsymbol{m}_{\mathbf{Cell}}$	For datasets with raw data, the measured cell weight was used. For external datasets, the cell weight was taken from datasheets.
$\boldsymbol{\Delta DOD}$	For datasets with raw data, the DOD was calculated by comparing the amount of charge per partial cycle with the capacity at the beginning of test. For external datasets, the value was extracted from the publication.
$\boldsymbol{Date}_{\mathbf{TX}}$	Date measurement X. $Date_{\mathrm{T2}} - Date_{\mathrm{T1}}$ calculates how many days are between measurements one and two.
$\boldsymbol{C}_{\mathbf{TX}}$	Capacity of measurement X. $(C_{\mathrm{T1}} - C_{\mathrm{T2}})$ calculates the capacity lost in between measurements one and two.
$\boldsymbol{\bar{U}}_{\mathbf{Cycle}}$	The average cycle voltage at cycling. For datasets with raw data, the value was extracted from the raw data by an integral mean value over the charge and discharge. For external datasets, this value was either extracted or approximated with the given mean SOC.

$\bar{I}_{\mathbf{Charge}}$	Charge current. For datasets with raw data, the value was extracted from the raw data by an integral mean value over the charge. For external datasets, this value was extracted from the information given in the publication.
$N_{\mathbf{FCE(EOT\|EOL)}}$	The counted equivalent full cycles based on $C_{\mathrm{Cell(BOL)}}$.
$\%_{\mathbf{Cap.Loss(EOT\|EOL)}}$	Marks the percentage points the cell reached at the closed data point at the EOL criteria.
$U_{\mathbf{nom}}$	The nominal cell voltage was read from datasheets.
$SOC_{\mathbf{Storage}}$	For datasets with raw data, this value was approximated by analyzing the storage voltage. For external datasets, this value was extracted from the publication.

Cyclical ENPOLITE Plot

The used raw data is initially filtered from outliers before calculating the cyclical ENPOLITE coefficients.

Detailed explanations of the evaluation can be found below.

Used specific energy cell (x-axis)

$$\frac{\Delta DOD\ * C_{\mathbf{Cell(BOL)}}\ * \bar{U}_{\mathbf{Cycle}}}{m_{\mathbf{Cell}}} = \frac{\mathbf{Wh}_{\mathbf{Cycle}}}{\mathbf{kg}}$$

With the cycling depth (DOD as depth of discharge) and the cell energy density, the used specific energy is calculated. It is based on the cell capacity at the beginning of life. Although the capacity changes with the cell lifetime, its position is not updated within the ENPOLITE plot. If the raw data is available, the cycling depth is calculated; if not, the cycling depth is taken from the publication.

Note: cells used with different cycle depths may have the same used specific energy. A cell with an energy density of 200 Wh/kg with a cycle depth of 50% and a cell with 125 Wh/kg and cycle depth of 80% have an equal used specific energy of 100 Wh/kg.

Used specific power cell (y-axis)

$$\frac{\bar{I}_{\mathbf{Charge}}\ * \bar{U}_{\mathbf{Cycle}}}{m_{\mathbf{Cell}}} = \frac{\mathbf{W}_{\mathbf{Charge}}}{\mathbf{kg}}$$

Only the mean charging current is used for the power calculations since it usually limits the cell lifetime performance.

Note: cells with different used C-Rates may have the same used specific power. This can be caused by differences in cell chemistry and the average cycle voltage.

Lifetime coefficient (circular area size)

The third coefficient (circular area size) is the linearized aging, expressed in energy throughput per percentage point of cell capacity lost, normalized to the respective cell weight.

$$\frac{\boldsymbol{N}_{\mathbf{FCE(EOT|EOL)}} * \boldsymbol{C}_{\mathbf{Cell(BOL)}} * \overline{\boldsymbol{U}}_{\mathbf{Cycle}}}{\boldsymbol{m}_{\mathbf{Cell}} * \ \%_{\mathbf{Cap.Loss(EOT|EOL)}}} = \frac{\mathbf{Wh}_{\mathbf{Throughput}}}{\mathbf{kg}\ * \%_{\mathbf{Cap.Loss}}}$$

For an accurate lifetime comparison, a lifetime coefficient was developed to compare cells with different sizes and chemistries while considering the actual normalized energy throughout every cell. The scheme below illustrates a comparison of three different cells and their corresponding lifetime coefficients.

Depending on the data availability, either the actual raw data is used to calculate the charge throughput or the throughput is estimated by multiplying the achieved equivalent full cycles and the cell rated capacity at the beginning of its aging test. The average cycle voltage is multiplied, and the overall coefficient is normalized to the cell mass and percentage point of capacity loss. Therefore, the formula above gives a fundamental approach to calculate the normalized energy throughput for sparse data availability.

For the figures given in this work, the degradation is fitted to a linear aging model to an EOL of 80% relative capacity.

For this, the first available capacity measurement beneath the 80% relative capacity mark was used. The latest available data point was used for cells that did not reach 80% relative capacity, and the capacity degradation was linearized upon that data point. The graphics given in the paper can be made with other EOL criteria lying above or beyond the 80% mark.

Besides a simple linear approximation of the aging curves, different approaches like a logarithmic or partial linear fitting, which we used for calendar aging, were considered. However, other models did overall not lead to a more accurate approximation for all datasets. Besides, these models have multiple parameters, which cannot be put in the one-dimensional circle area.

The figure below illustrates the advantages of the lifetime coefficient compared to a typical aging plot. For simplicity, capacity instead of energy was used. It compares three theoretical cells with different weights and energy densities, illustrating which cells have the same lifetime coefficient. Cell A has five times the weight, but the same energy density as Cell B; both degrade the same when normalized to weight. Cell C is the same weight and has the same aging gradient as Cell B, but the lifetime coefficient is lower with a lower energy density.

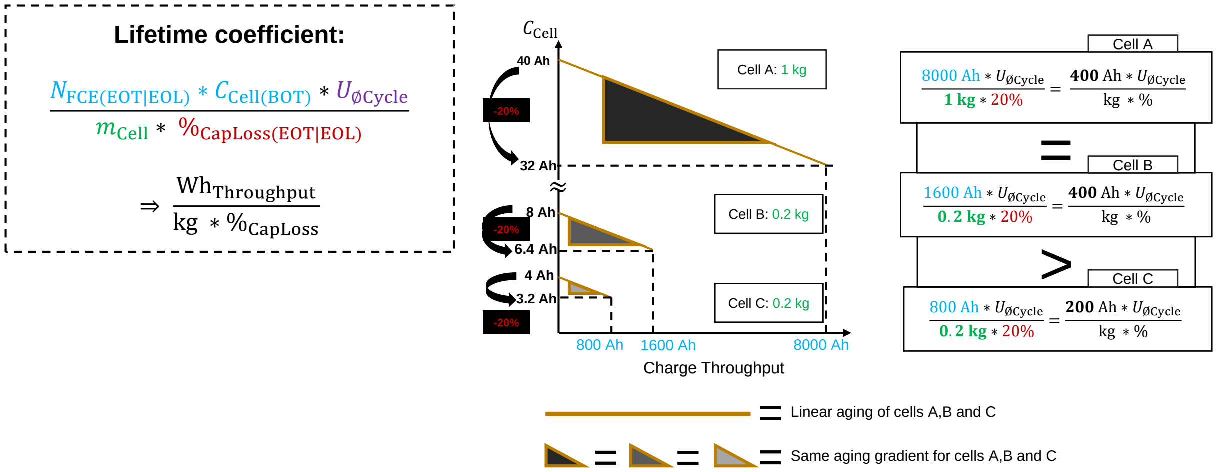

Cyclical ENPOLITE Plot: Inserting one exemplary cell

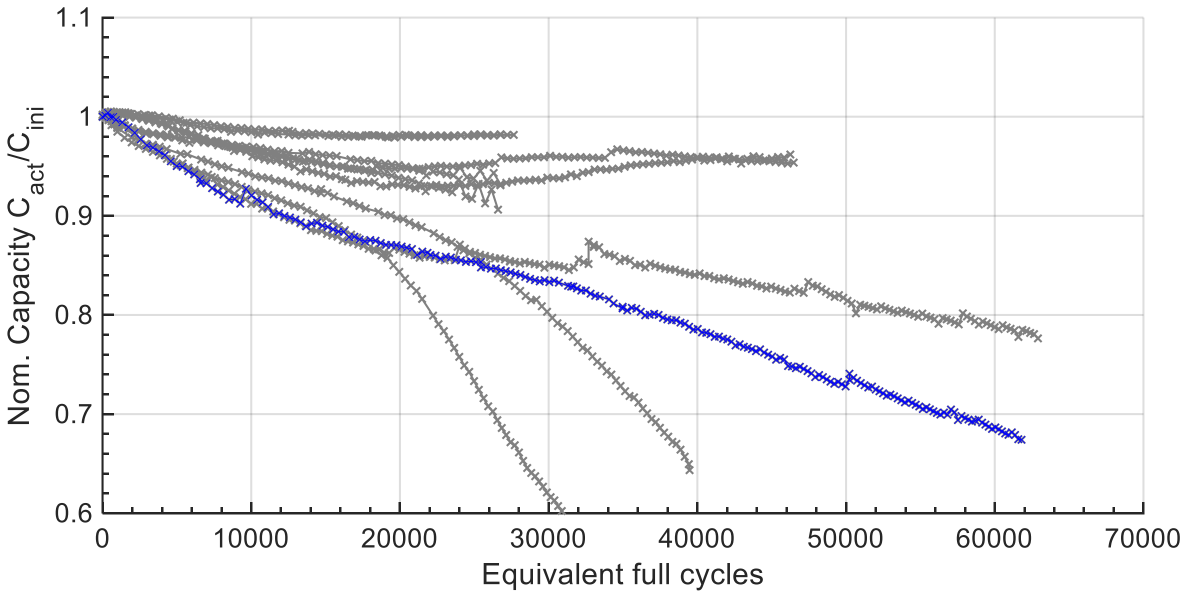

The results of a cycle aged dataset can be illustrated with the relative capacity changing over the reached equivalent full cycles. Every single cross stands for one Check-Up within the aging test. The blue cell and its respective aging test results are inserted into the ENPOLITE Plot step by step.

The X-value (used specific energy)

$$\frac{\boldsymbol{\Delta DOD} \; * \, \boldsymbol{C_{\mathrm{Cell(BOL)}}} \; * \, \boldsymbol{\overline{U}_{\mathrm{Cycle}}}}{\boldsymbol{m_{\mathrm{Cell}}}} = \frac{\mathbf{Wh_{Cycle}}}{\mathbf{kg}}$$

In the following, the different parameters and their extraction assumptions are explained in detail.

The cell mass is 150.8 g or 0.15 kg.

Parameter	Value
m_{cell}	0.15 kg

$C_{\mathrm{Cell(BOL)}}$: For datasets with raw data, this is the first extractable discharge capacity for every individual cell. For external datasets, the first measured capacity, which was sometimes the charge and sometimes the discharge capacity, was extracted. Often this was the 1C discharge capacity. For external datasets, with only an aging diagram, the cell nominal capacity was used.

Since raw data was given for this dataset, this cell's measured first discharge capacity was available. For this cell, the used capacity is $C_{\mathrm{Cell(BOL)}} = 3.16\ \mathrm{Ah}$.

Parameter	Value
m_{cell}	0.15 kg
$C_{\mathrm{Cell(BOL)}}$	3.16 Ah

ΔDOD: For datasets with raw data, the DOD was calculated by comparing the amount of charge per partial cycle with the capacity mentioned above at the beginning of the test. For external datasets, the value was extracted from the publication.

To further explain the extraction process, the following raw data cycles are observed in the figure below:

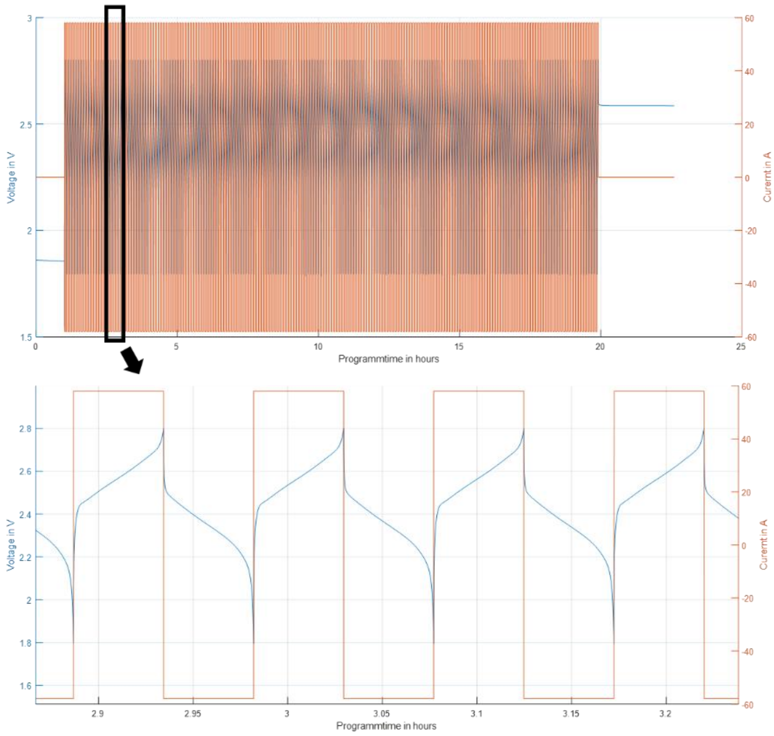

For this specific aging test, constant current cycling (Constant current charge and discharge) was used to charge and discharge.

In the next figure, data points at the beginning and end of charging and discharging are marked.

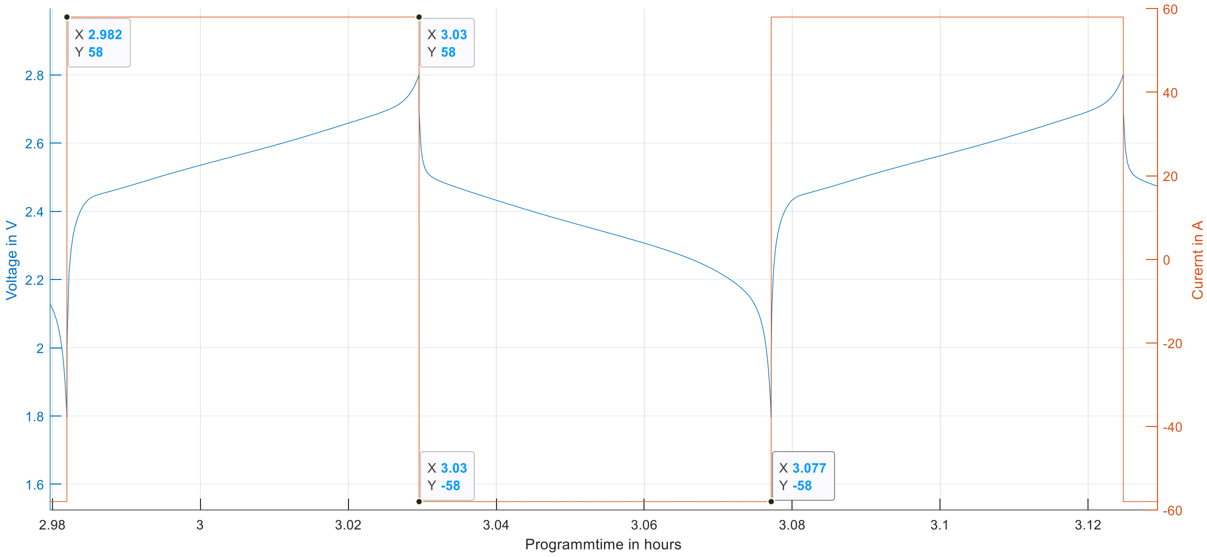

For an exemplary cycle, the amount of charge that went through the cell was counted using the actual battery current and its time duration:

For the charging phase: $(3.03h - 2.982h) * 58A \approx 2.78Ah \Leftrightarrow \frac{2.78Ah}{3.16Ah} \approx 0.88$ cycle depth

Discharging phase: $|(3.077h - 3.03h) * (-58A)| \approx 2.73Ah \Leftrightarrow \frac{2.73Ah}{3.16Ah} \approx 0.86$ cycle depth

The first 20-200 cycles were used to minimize the impact from data outliers, and the calculated cycle depth was averaged afterward. For the observed cell, this results in a $\Delta DOD = 0.87$

Parameter	Value
$\boldsymbol{m_{cell}}$	0.15 kg
$\boldsymbol{C_{\mathrm{Cell(BOL)}}}$	3.16 Ah
$\boldsymbol{\Delta DOD}$	0.87

$\overline{U}_{\mathrm{Cycle}}$: This value was extracted from the raw data by an integral mean value over the charge or discharge voltage curve for raw data datasets. This value was either directly extracted from the publication or approximated with the given mean SOC for external datasets.

For illustration, the battery voltage while charging and discharging is further examined:

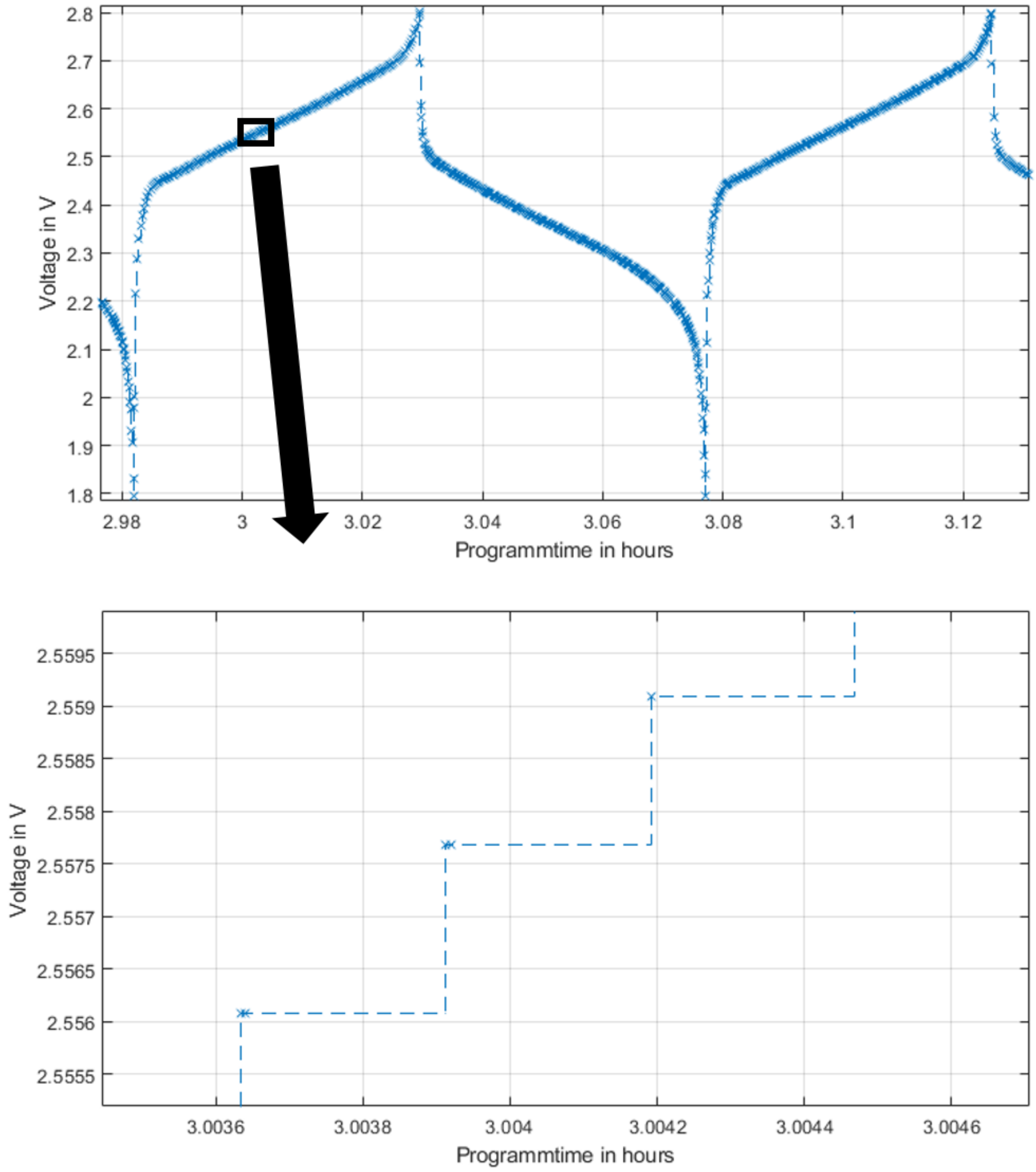

The raw voltage data were reproduced into a step function to extract the mean voltage. Therefore different voltage levels and time durations of these voltage levels are given. To further determine the mean cycle voltage, the following calculation was executed:

$$\frac{\sum U_{level} * \Delta t_{level}}{t_{charge}} \text{ resp. } \frac{\sum U_{level} * \Delta t_{level}}{t_{discharge}}$$

This was calculated throughout and for the entire cycling process.

Lastly, the overall mean from the mean charge voltage and mean discharge voltage was formed, which for this cell was: 2.46V

Parameter	Value
$\boldsymbol{m_{cell}}$	0.15 kg
$\boldsymbol{C_{\mathrm{Cell(BOL)}}}$	3.16 Ah
$\boldsymbol{\Delta DOD}$	0.87
$\boldsymbol{\overline{U}_{\mathrm{Cycle}}}$	2.46 V

Afterward, the x-coefficient (used specific energy) can be calculated:

$$\frac{\Delta DOD \;*\; C_{\text{Cell(BOL)}} \;*\; \bar{U}_{\text{Cycle}}}{m_{\text{Cell}}} = \frac{\mathbf{Wh_{Cycle}}}{\mathbf{kg}}$$

$$\frac{0.87 * 3.16\text{Ah} \;*\; 2.46\text{V}}{0.15\text{kg}} \approx \mathbf{45}\,\frac{\mathbf{Wh_{Cycle}}}{\mathbf{kg}}$$

The Y-value (used specific power)

$$\frac{\bar{\mathbf{I}}_{\mathbf{Charge}} \;*\; \bar{\mathbf{U}}_{\mathbf{Cycle}}}{\mathbf{m_{Cell}}} = \frac{\mathbf{W_{Charge}}}{\mathbf{kg}}$$

$\bar{I}_{\text{Charge}}$ This value was extracted from the raw data by an integral mean value over the charge current for raw data. For external datasets, this value was extracted from the information given in the publication.

Note: If raw data is available, the whole charging process is taken into account, including the slower CC/CV at the end of a cycle if, for example, a cell was cycled at 100% cycle depth.

Only the mean charging current was used for power calculations since it is usually limiting lifetime performance. For the observed cell aging test conditions, the extractable charging current can be directly read from the figure below since a constant current charging profile was used.

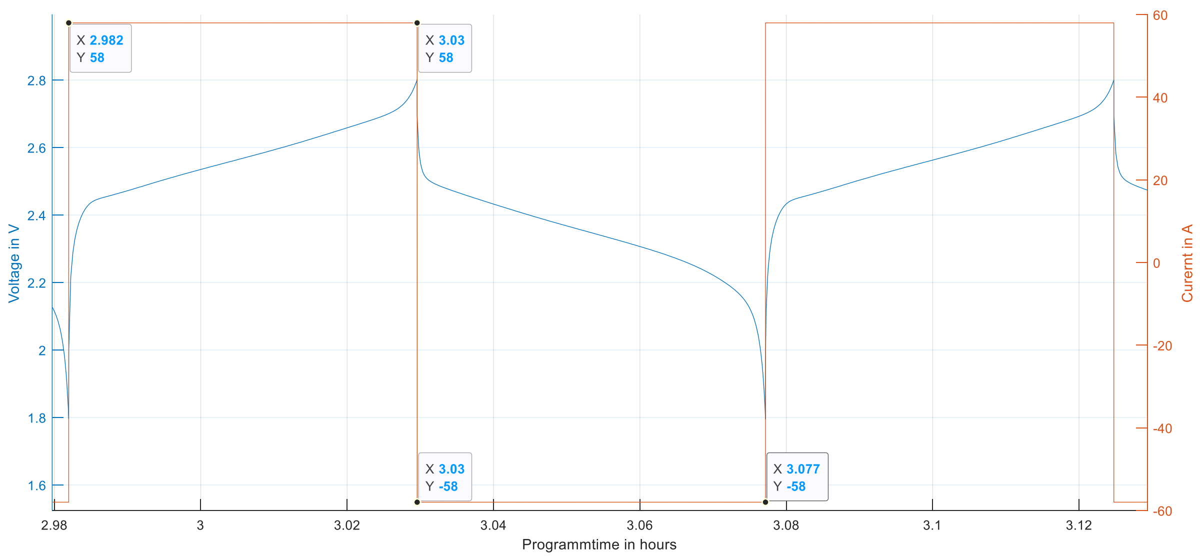

If there is no constant current cycling, the average current is formed from the measured charge throughput divided by the charging time.

In this example, the mean charge current is 58A.

Parameter	Value
$\boldsymbol{m_{cell}}$	0.15 kg
$\boldsymbol{C}_{\mathbf{Cell(BOL)}}$	3.16 Ah
$\Delta\boldsymbol{DOD}$	0.87
$\overline{\boldsymbol{U}}_{\mathbf{Cycle}}$	2.46 V
$\overline{\boldsymbol{I}}_{\mathbf{Charge}}$	58A

Afterward, the used specific power can be calculated as:

$$\frac{\overline{\boldsymbol{I}}_{\mathbf{Charge}} * \overline{\boldsymbol{U}}_{\mathbf{Cycle}}}{\boldsymbol{m}_{\mathbf{Cell}}} = \frac{\mathbf{W}_{\mathbf{Charge}}}{\mathbf{kg}}$$

$$\frac{58\mathrm{A} * 2.46\mathrm{V}}{0.15\mathrm{kg}} \approx \mathbf{945}\frac{\mathbf{W}_{\mathbf{Charge}}}{\mathbf{kg}}$$

The Bubble size (lifetime coefficient)

$$\frac{\boldsymbol{N}_{\mathbf{FCE(EOT|EOL)}} * \boldsymbol{C}_{\mathbf{Cell(BOL)}} * \overline{\boldsymbol{U}}_{\mathbf{Cycle}}}{\boldsymbol{m}_{\mathbf{Cell}} * \%_{\mathbf{Cap.Loss(EOT|EOL)}}} = \frac{\mathbf{Wh}_{\mathbf{Throughput}}}{\mathbf{kg} * \%_{\mathbf{Cap.Loss}}}$$

$\boldsymbol{N}_{\mathbf{FCE(EOT|EOL)}}$ is the counted equivalent full cycles based on the capacity $C_{\mathrm{Cell(BOL)}}$ mentioned above.

$\%_{\mathbf{Cap.Loss(EOT|EOL)}}$ marks the percentage points the cell has reached at the closest data point to the defined EOL criteria.

The counted equivalent full cycles can be recalculated from the charge throughput given in the raw data or, for this example, just read from the graphic below.

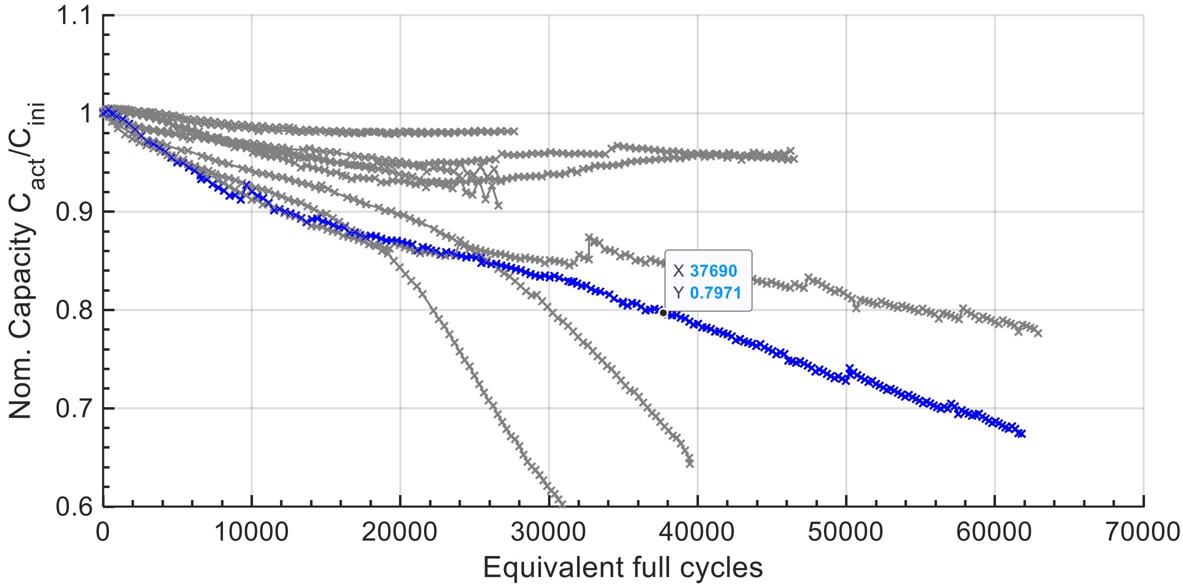

It can be seen that the first data point, which is below 80% nominal capacity, is at 37690 EFC and at 79.7% relative remaining capacity, which means the observed cell has lost 20.3% of its relative capacity.

Parameter	Value
m_{cell}	0.15 kg
$C_{\mathrm{Cell(BOL)}}$	3.16 Ah
ΔDOD	0.87
$\bar{U}_{\mathrm{Cycle}}$	2.46 V
$\bar{I}_{\mathrm{Charge}}$	58A
$N_{\mathrm{FCE(EOT\|EOL)}}$	37690
$\%_{\mathrm{Cap.Loss(EOT\|EOL)}}$	20.3%

Afterward, the lifetime coefficient can be calculated:

$$\frac{N_{\mathrm{FCE(EOT|EOL)}} * C_{\mathrm{Cell(BOT)}} * \bar{U}_{\mathrm{Cycle}}}{m_{\mathrm{Cell}} * \%_{\mathrm{Cap.Loss(EOT|EOL)}}} = \frac{\mathbf{Wh_{Throughput}}}{\mathbf{kg} * \%_{\mathbf{Cap.Loss}}}$$

$$\frac{37690 * 3.16\mathrm{Ah} * 2.46\mathrm{V}}{0.15\mathrm{kg} * 20.3\%} \approx \mathbf{100000}\frac{\mathbf{Wh_{Throughput}}}{\mathbf{kg} * \%_{\mathbf{Cap.Loss}}}$$

All three coefficients and their calculations are combined in the figure below.

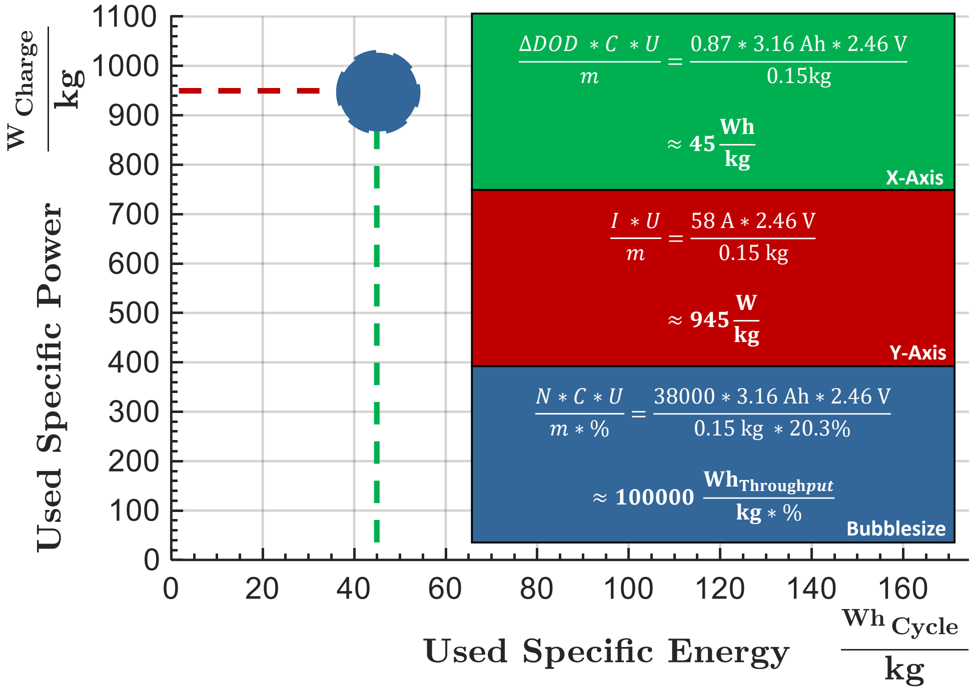

The lifetime coefficient is reflected as the area size in the ENPOLITE Plot. The figure below gives an example of this.

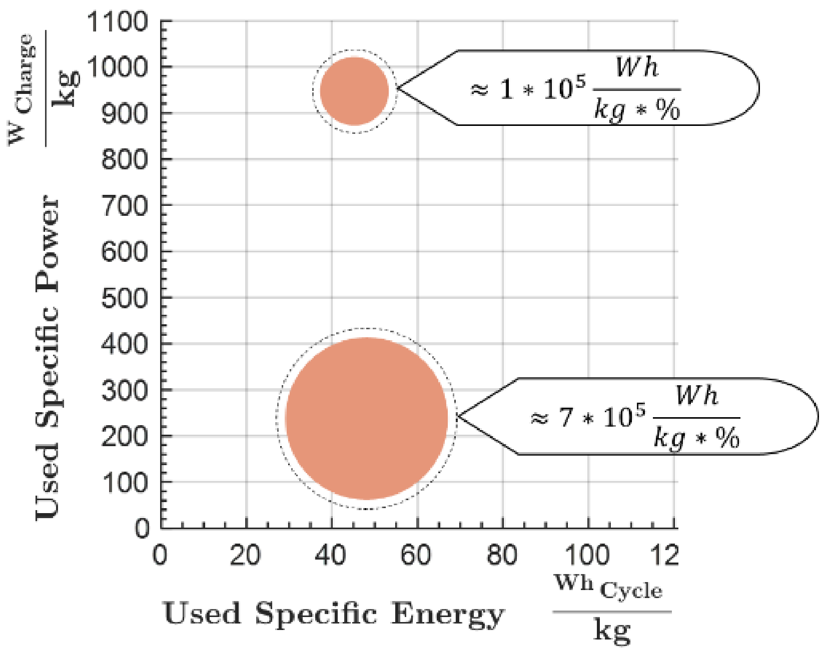

Lastly, the mean cycling temperature is extracted as a simple mean value. It is reflected as the circumference color of every circle data point. One whole dataset, including all parameters, can be seen in the figure below.

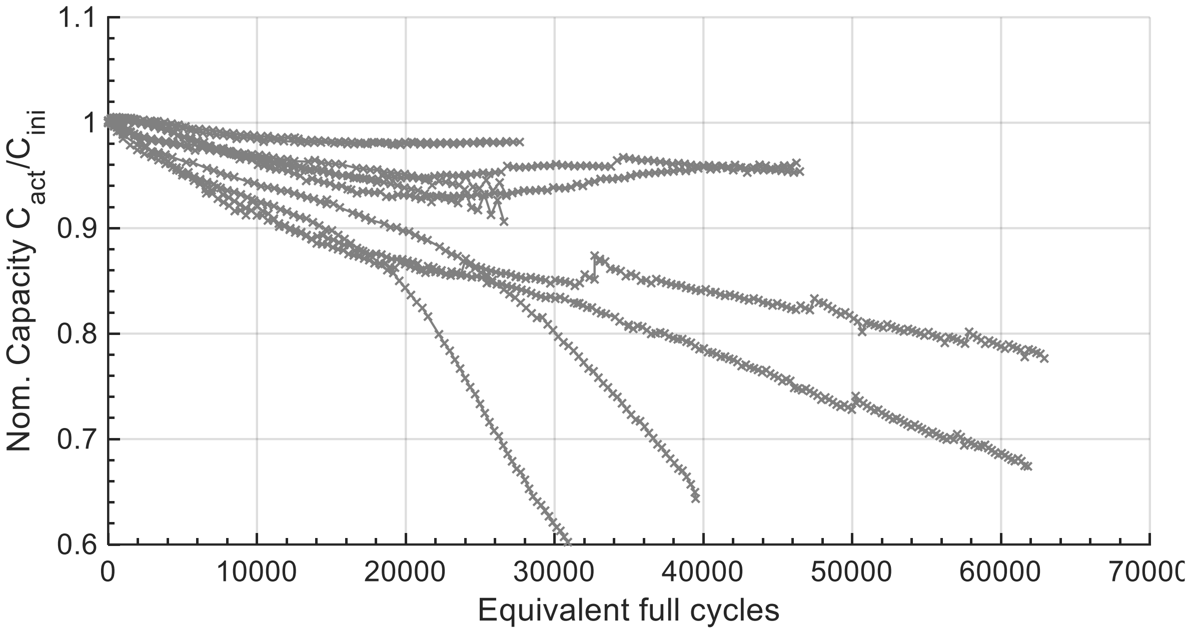
1.1
1
0.9
0.8
0.7
0.6
Nom. Capacity C_{act}/C_{ini}
0
10000
20000
30000
40000
50000
60000
70000
Equivalent full cycles

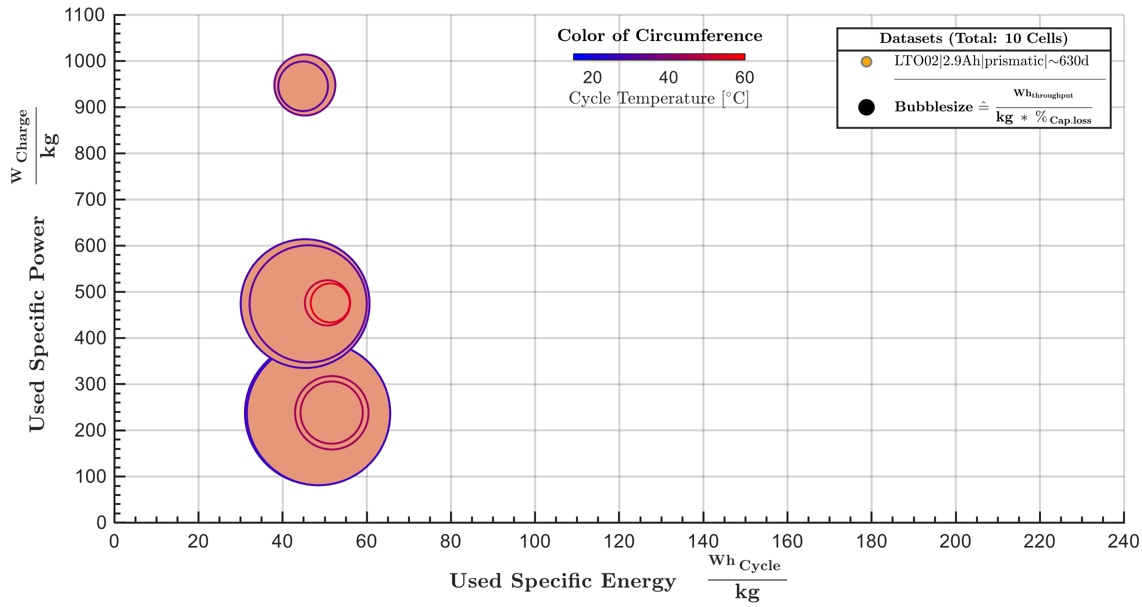

Color of Circumference
20
40
60
Cycle Temperature [°C]
Datasets (Total: 10 Cells)
LTO02|2.9Ah|prismatic|~630d
Bubblesize ≙ Wh_throughput / kg * %_Cap.loss
Used Specific Power W_Charge / kg
Used Specific Energy Wh_Cycle / kg
0
100
200
300
400
500
600
700
800
900
1000
1100
0
20
40
60
80
100
120
140
160
180
200
220
240

Cyclical ENPOLITE Plot: Overview of Cells

An interactive version of the cell overview can be found in the Supporting Information online.

783 individual battery cells from 17 datasets are shown in the ENPOLITE plot of this work. Each data point represents a cyclic aging test of a cell within a dataset. Yellow crosses depict NMC|NCA cathode battery cells and show a wide range of operation points in the *Used Specific Energy*, while LTO-datasets with blue crosses are mainly aged at high *Used Specific Power,* and LFP with green crosses lie in between. The legend shows relevant metadata (cell chemistry, nominal capacity, cell format, and test duration) for each record, which uniquely associates this record with the table in the appendix to obtain detailed information on the cells used in each case.

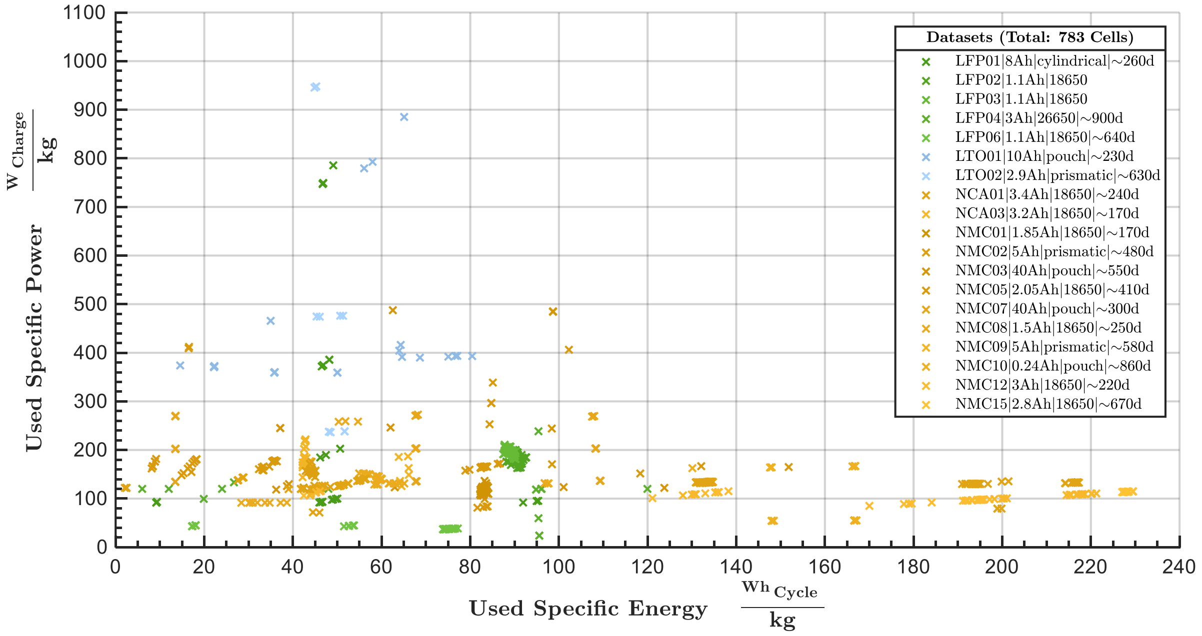

Volumetric Cyclical ENPOLITE Plot:

Here the Cyclical ENPOLITE Plot is shown, but relative to the cell volume not weight. If the volume was not part of the cell datasheet, the volume of the enclosing cyclinder was used for the cylindrical cells. For pouch and prismatic cells without datasheet volume, the volume of the enclosing cuboid was calculated.

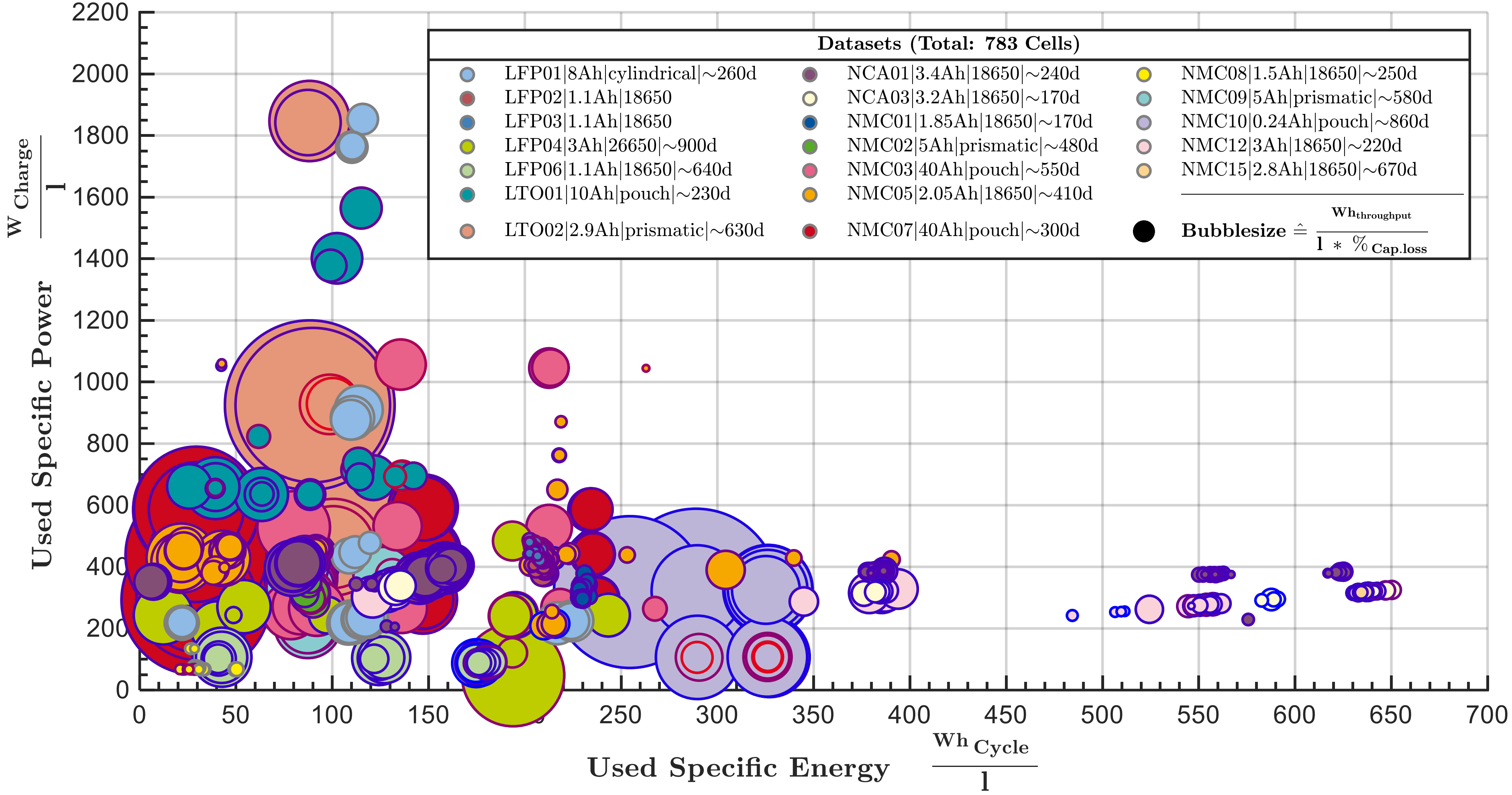

Datasets (Total: 783 Cells)
LFP01|8Ah|cylindrical|~260d
LFP02|1.1Ah|18650
LFP03|1.1Ah|18650
LFP04|3Ah|26650|~900d
LFP06|1.1Ah|18650|~640d
LTO01|10Ah|pouch|~230d
LTO02|2.9Ah|prismatic|~630d
NCA01|3.4Ah|18650|~240d
NCA03|3.2Ah|18650|~170d
NMC01|1.85Ah|18650|~170d
NMC02|5Ah|prismatic|~480d
NMC03|40Ah|pouch|~550d
NMC05|2.05Ah|18650|~410d
NMC07|40Ah|pouch|~300d
NMC08|1.5Ah|18650|~250d
NMC09|5Ah|prismatic|~580d
NMC10|0.24Ah|pouch|~860d
NMC12|3Ah|18650|~220d
NMC15|2.8Ah|18650|~670d
Bubblesize ≙ Wh_throughput / l * %_Cap.loss
Used Specific Power W_Charge / l
Used Specific Energy Wh_Cycle / l
0
200
400
600
800
1000
1200
1400
1600
1800
2000
2200
0
50
100
150
250
300
350
400
450
500
550
600
650
700

Calendar ENPOLITE Plot

The used evaluated raw data was initially cleared from general data outliers before calculating the calendar ENPOLITE coefficients.

Detailed explanations of the evaluation for all the different cell sizes can be found further below.

Used specific storage energy (x-axis)

$$\frac{\boldsymbol{C}_{\mathbf{Cell(BOL)}} * \boldsymbol{U}_{\mathbf{nom}} * \boldsymbol{SOC}_{\mathbf{Storage}}}{\boldsymbol{m}_{\mathbf{Cell}}} = \frac{\mathbf{Wh_{SOC}}}{\mathbf{kg}}$$

Note: Cells with a storage SOC of 0% are mapped at $0\ \frac{Wh_{SOC}}{kg}$ *in the calendar ENPOLITE Plot*

This coefficient describes the stored energy during the aging normalized to the weight of the cell. Due to data availability, $\mathrm{U_{nom}}$ was used instead of the integrated mean storage voltage. Most of the datasets used in the calendar ENPOLITE Plot are from extracted aging diagrams where often just the storage SOC is given. The used approximation for the stored specific energy considers differences in cell chemistry and the respective storage SOC and could be evaluated for sets with incomplete data.

Test Temperature in °C (y-axis)

The y-axis coefficient is not further modified and results from the cells' storage temperature in °C.

Lifetime coefficient (circular area size)

The third coefficient (circular area size) corresponds to the number of days until a cell has lost the energy density of $1\,\frac{Wh}{kg}$.

$$\frac{\boldsymbol{Date}_{\mathbf{T2}} - \boldsymbol{Date}_{\mathbf{T1}}}{\frac{(\boldsymbol{C}_{\mathbf{T1}} - \boldsymbol{C}_{\mathbf{T2}}) * \boldsymbol{U}_{\mathbf{nom}}}{\boldsymbol{m}_{\mathbf{Cell}}}} = \frac{\mathbf{Days}}{\frac{\mathbf{Wh_{Lost}}}{\mathbf{kg}}}$$

For the representation of the calendar lifetime data, however, some striking differences have to be considered. Particularly in calendar aging tests, cells are sometimes still over 100% of their initial capacity even after longer aging periods of more than 2 years. However, an increase in the aging process's capacity leads to a negative value by definition of the used aging coefficient according to the formula above. For this reason, the value ∞ has been inserted into the calendar ENPOLITE-Plot. It does not infer the cell lives forever but represents the aging of lifetime coefficient results, which cannot yet be evaluated or quantified because the corresponding cells' capacities are still rising. The circle area's size is fixed and does not represent an absolute meaning but shows an exceptional lifetime's operating points.

The scheme below again shows some exemplary cells for calculating the lifetime coefficient illustrating the advantages of regular aging diagrams. It compares three theoretical cells with different weights and aging gradients, illustrating which cells have the same lifetime coefficient. Cell A has five times the weight and the same aging gradient as cell B. But cell B loses more capacity per day, and 5 cells of type B would still only work for 160 days; the lifetime coefficient of cell A is better than B. Cell C is half the weight of cell B and has a slower aging gradient. Therefore it has a better aging coefficient than B and the same as A. For simplification reasons, the voltage was considered as constant in this scheme. In actual usage, the voltage is another critical parameter in which the cell lifetime rating may be distinguished.

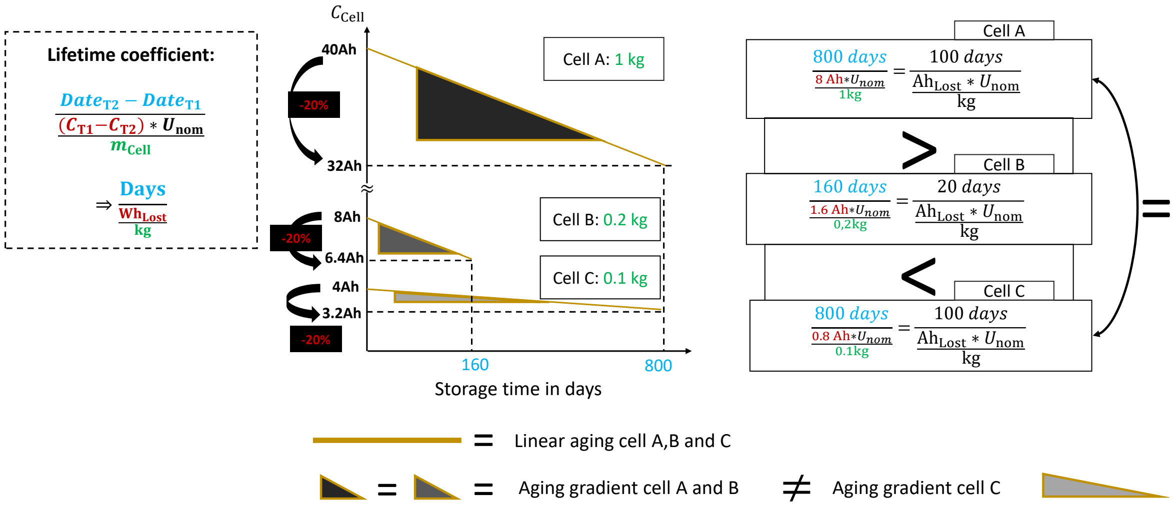

Deep dive into the linear aging model of the calendar lifetime coefficient

In contrast to the lifetime coefficient used for the cyclical ENPOLITE Plot, a different approach was used for the calendar case. A partial linear fitting was used to exclude the common reversible aging phenomena due to the anode overhang. For this, only the best linear fitting part of the capacity degradation was calculated.

Since the duration in which the reversible aging takes place varies in different circumstances, initially, the first 90 days of the respective aging test are not used when calculating the lifetime coefficient. Afterward, various possible linear aging degradation curves are created with the constraint that at least 50% of the remaining data points are included in the linear fit. Afterward, the fit with the highest coefficient of determination is selected.

If the overall data points without the first 90 days of aging are less than four for a cell, the fit is executed with every remaining data point.

The figure below illustrates an example of this procedure.

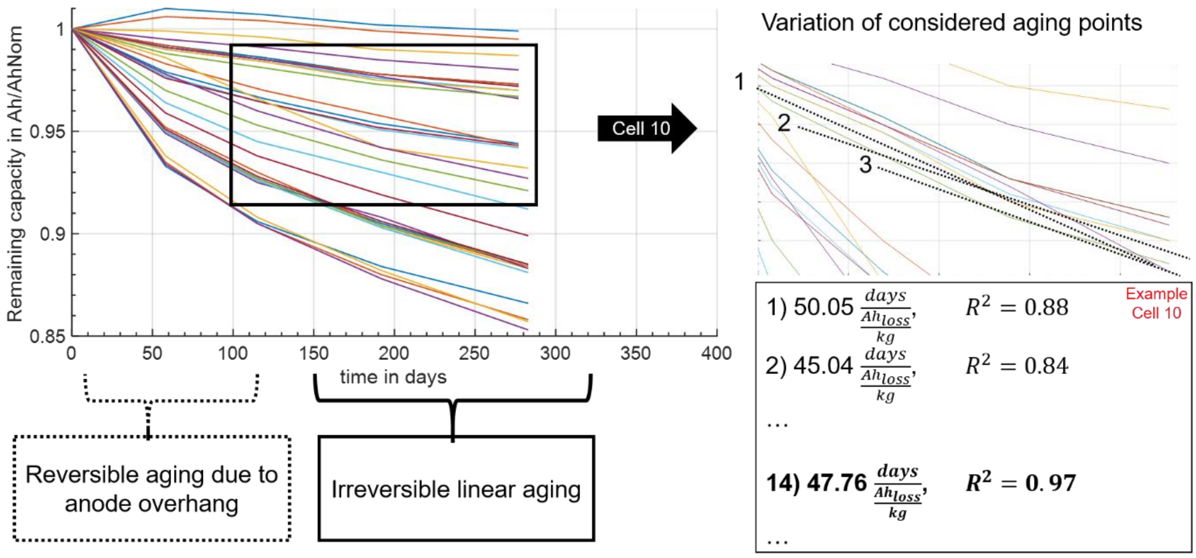

Calendar ENPOLITE Plot: Inserting one exemplary cell

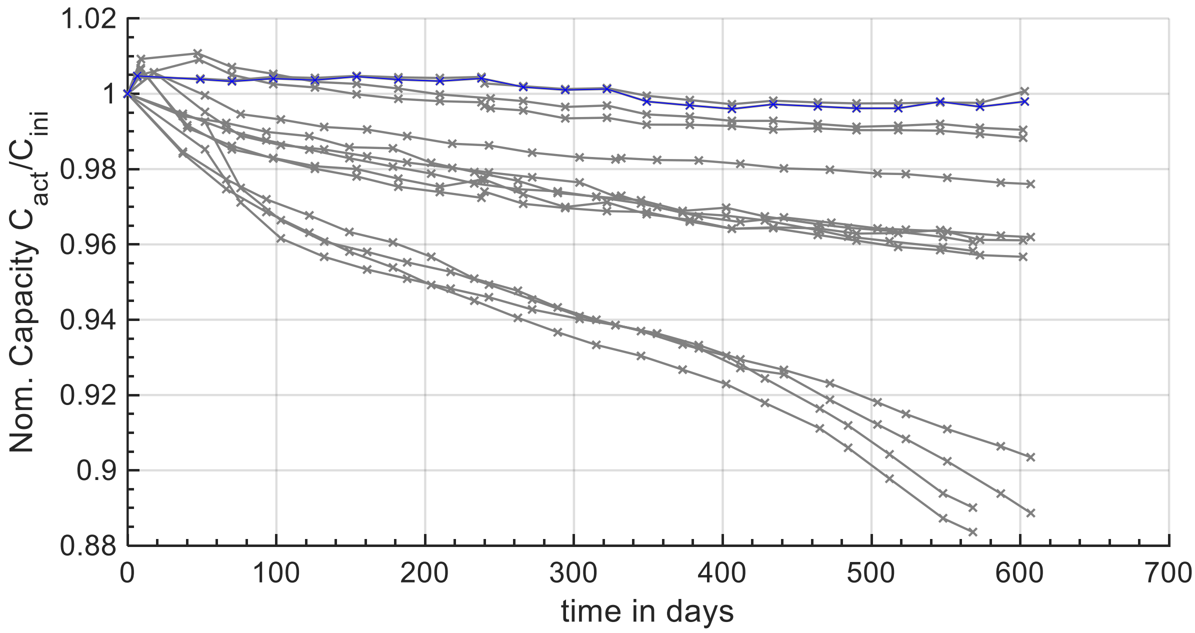

Calendar aged dataset results can be illustrated with the relative capacity changing over the number of storage days. Every single cross stands for one Check-Up within the aging test. The blue cell and its respective aging test results are inserted into the ENPOLITE Plot step by step.

The X-value (stored specific energy)

$$\frac{C_{\mathrm{Cell(BOT)}} * U_{\mathrm{nom}} * SOC_{\mathrm{Storage}}}{m_{\mathrm{Cell}}} = \frac{\mathrm{Wh_{SOC}}}{\mathrm{kg}}$$

In the following, the different parameters and the assumptions used are explained in detail.

The cell mass is 150.7 g or around 0.15 kg.

Parameter	Value
m_{cell}	0.15 kg

$C_{\mathrm{Cell(BOL)}}$: For datasets with raw data, this is the first extractable full discharge capacity for every individual cell. For external datasets, the first measured capacity, which was sometimes the charge and sometimes the discharge capacity, was extracted. Usually, this was the 1C discharge capacity. For external datasets, which only had an aging chart, the cell nominal capacity was used.

Since raw data was given for this dataset, this cell's measured first discharge capacity was available. For this cell, the extracted capacity was $C_{\mathrm{Cell(BOL)}} = 3.17\ \mathrm{Ah}$.

Parameter	Value
m_{cell}	0.15 kg
$C_{\mathrm{Cell(BOL)}}$	3.17 Ah

U_{nom}: This value was extracted from datasheets.

Due to data availability the $\mathrm{U_{nom}}$ instead of the integrated mean storage voltage was used to calculate the specific stored energy. Most of the datasets used in the calendar ENPOLITE Plot are from extracted aging diagrams where often just the storage SOC is given. SOC is not equal to State-Of-Energy (SOE), but with the nominal voltage, the error can be diminished, considering differences in cell chemistry.

For the exemplary cell, the nominal voltage is $U_{\mathrm{nom}} = 2.45$ V

Parameter	Value
m_{cell}	0.15 kg
$C_{\mathrm{Cell(BOL)}}$	3.17 Ah
U_{nom}	2.45 V

SOC_{Storage}: For raw datasets, this value was approximated by analyzing the storage voltage and the open-circuit voltage measurement at the beginning of a check-up procedure. For external datasets, this value was extracted from the publication.

For further explanations of the approximation done in the raw data case, the figure below shows one Check-Up procedure consisting of a capacity check and pulse currents for the observed cell's impedance estimation.

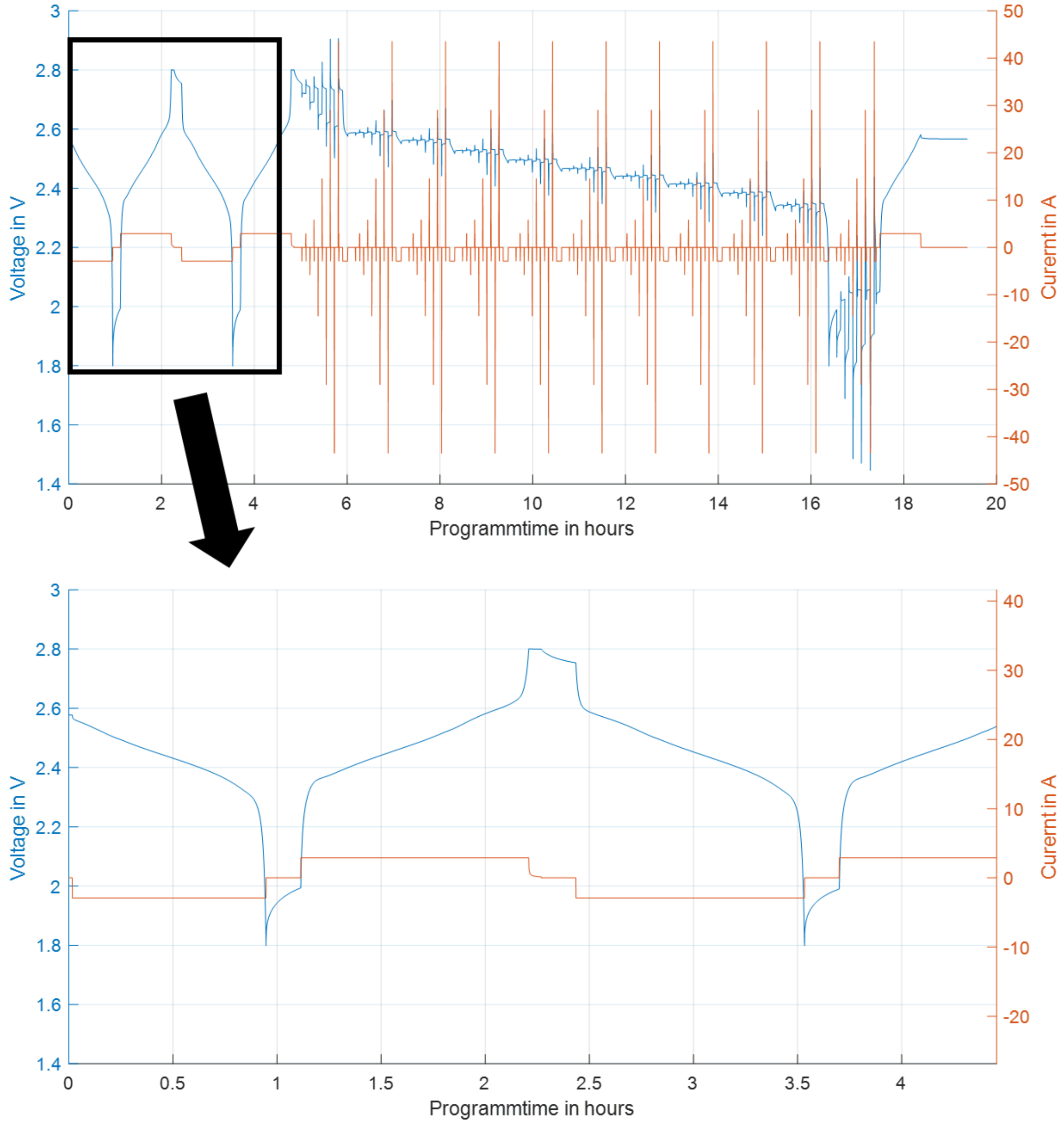

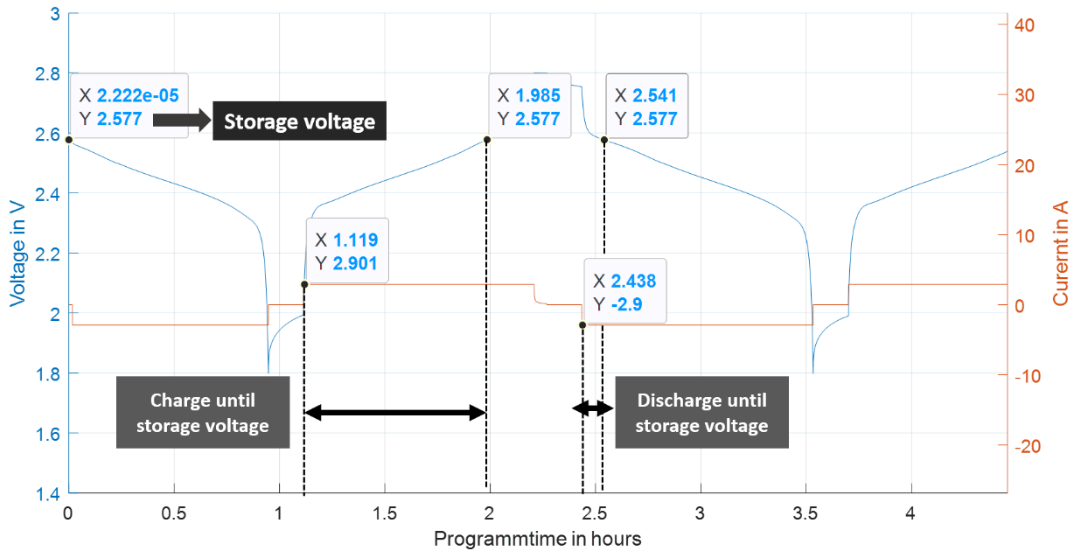

The storage SOC is determined by comparing the voltage level at storage (beginning of check-up) to the voltage curve during charging and discharging while counting the charge and discharge throughput:

For charging phase: $\frac{(t_{CHA_{start}} - t_{U=2.58V}) * I_{CHA}}{C_{CHA}} = \frac{(1.99h - 1.12h) * 2.90A}{3.17Ah} \approx 0.79$

Discharging phase: $1 - \frac{(t_{DSC_{start}} - t_{U=2.58V}) * I_{dsc}}{C_{DCH}} = 1 - \frac{|(2.54h - 2.44h) * (-2.9A)|}{3.17Ah} \approx 0.91$

Note: The used charge capacity C_{cha} is different from the used discharge capacity C_{dch}. Both values change for every check-up and are used separately for every charge/discharge phase to guarantee an accurate estimate for the storage SOC

Afterward, the mean out of both values gives the first estimated storage SOC.

To get the most accurate result, this storage SOC is calculated throughout the entire storage time. Lastly, the mean value from the test series is used for further calculations. For this cell SOC_{Storage} = 0.85

Parameter	Value
$\boldsymbol{m_{cell}}$	0.15 kg
$\boldsymbol{C_{\text{Cell(BOL)}}}$	3.17 Ah
$\boldsymbol{U_{\text{nom}}}$	2.45 V
$\boldsymbol{SOC_{\text{Storage}}}$	0.85

With these four parameters, the x-coefficient can now be calculated:

$$\frac{\boldsymbol{C_{\text{Cell(BOT)}} * U_{\text{nom}} * SOC_{\text{Storage}}}}{\boldsymbol{m_{\text{Cell}}}} = \frac{\mathbf{Wh_{SOC}}}{\mathbf{kg}}$$

$$\frac{3.17\mathrm{Ah} * 2.45\mathrm{V} * 0.85}{0.15\mathrm{kg}} \approx \mathbf{44}\,\frac{\mathbf{Wh_{SOC}}}{\mathbf{kg}}$$

The Y-value (storage temperature in °C)

This value is directly extracted from the aging test datasheets. For this cell, the storage temperature is 25°C.

The bubble size (lifetime coefficient)

$$\frac{\boldsymbol{Date}_{\mathbf{T2}} - \boldsymbol{Date}_{\mathbf{T1}}}{\frac{(\boldsymbol{C}_{\mathbf{T1}} - \boldsymbol{C}_{\mathbf{T2}}) * \boldsymbol{U}_{\mathbf{nom}}}{\boldsymbol{m}_{\mathbf{Cell}}}} = \frac{\mathbf{Days}}{\frac{\mathbf{Wh_{Lost}}}{\mathbf{kg}}}$$

Further details on the calculation can be found in the first part of the supplementary material.

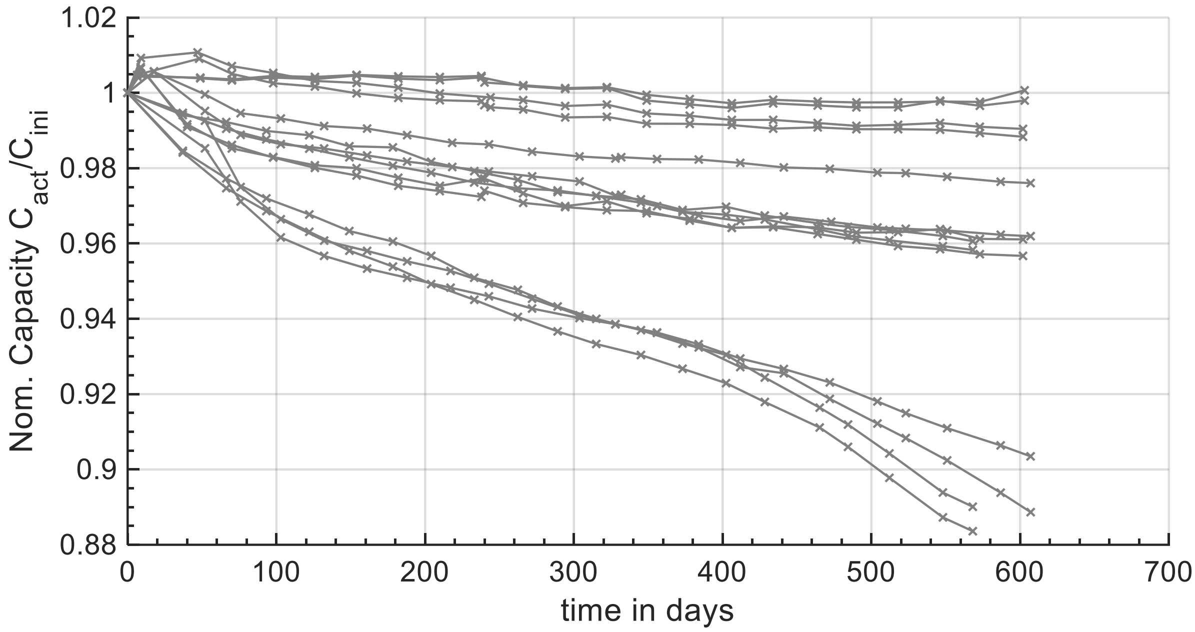

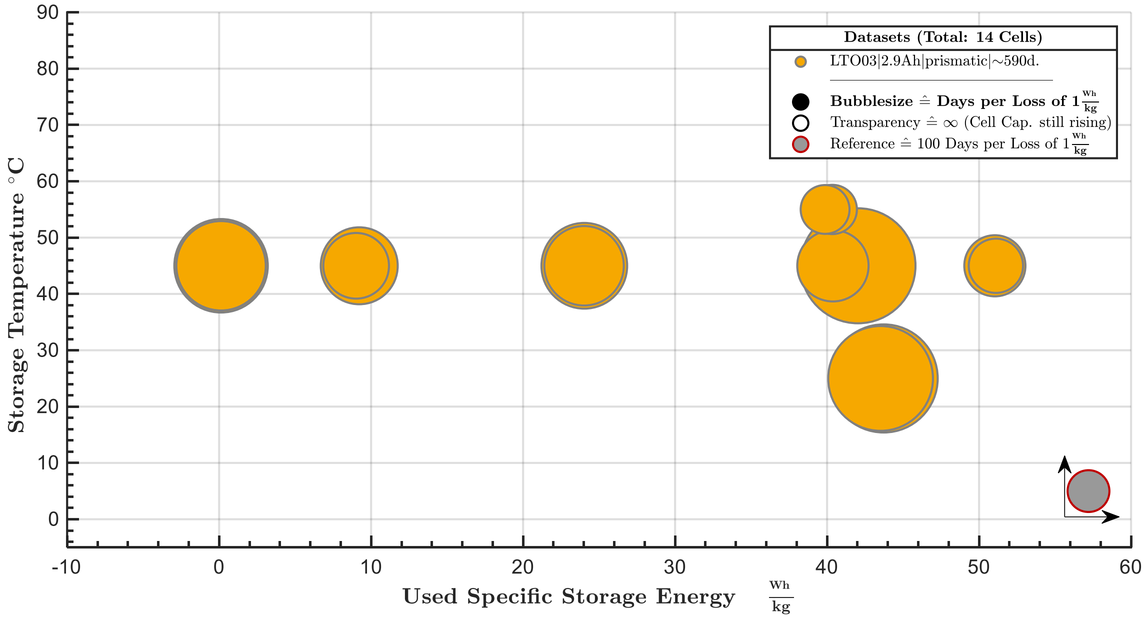
Datasets (Total: 14 Cells)
LTO03|2.9Ah|prismatic|~590d.
Bubblesize ≙ Days per Loss of 1 Wh/kg
Transparency ≙ ∞ (Cell Cap. still rising)
Reference ≙ 100 Days per Loss of 1 Wh/kg
Storage Temperature °C
90
80
70
60
50
40
30
20
10
0
-10
0
10
20
30
40
50
60
Used Specific Storage Energy Wh/kg

Calendar ENPOLITE Plot: Overview of Cells

An interactive version of the cell overview can be found in the Supporting Information online.

The plot below shows 307 battery cells from 11 datasets. Each cross stands for a calendar aging test of a cell. Yellow crosses are NMC|NCA cathode battery cells and show a wide range of operation points in the *Stored Specific Energy*. LTO-Datasets are aged at lower *Stored Specific Energy*. LFP lies in between. The legend shows metadata (cell chemistry, nominal capacity, cell format, test duration) for each record, which uniquely associates this record with the table in the appendix.

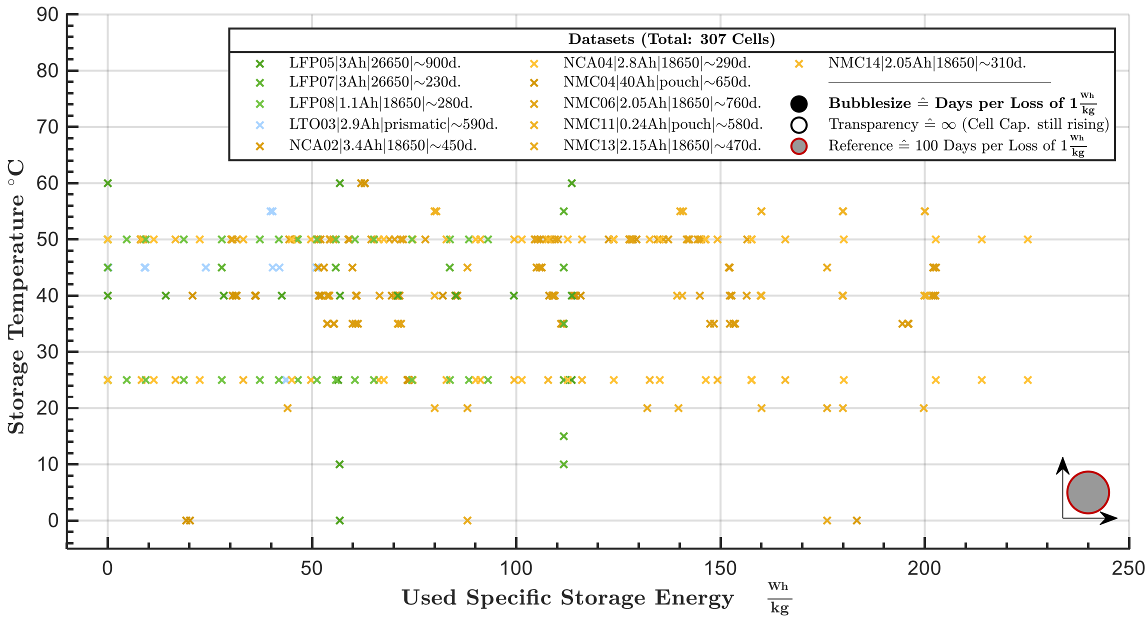

Volumetric Calendar ENPOLITE Plot:

Here the Calendar ENPOLITE Plot is shown, but relative to the cell volume not weight. If the volume was not part of the cell datasheet, the volume of the enclosing cyclinder was used for the cylindrical cells. For pouch and prismatic cells without datasheet volume, the volume of the enclosing cuboid was calculated.

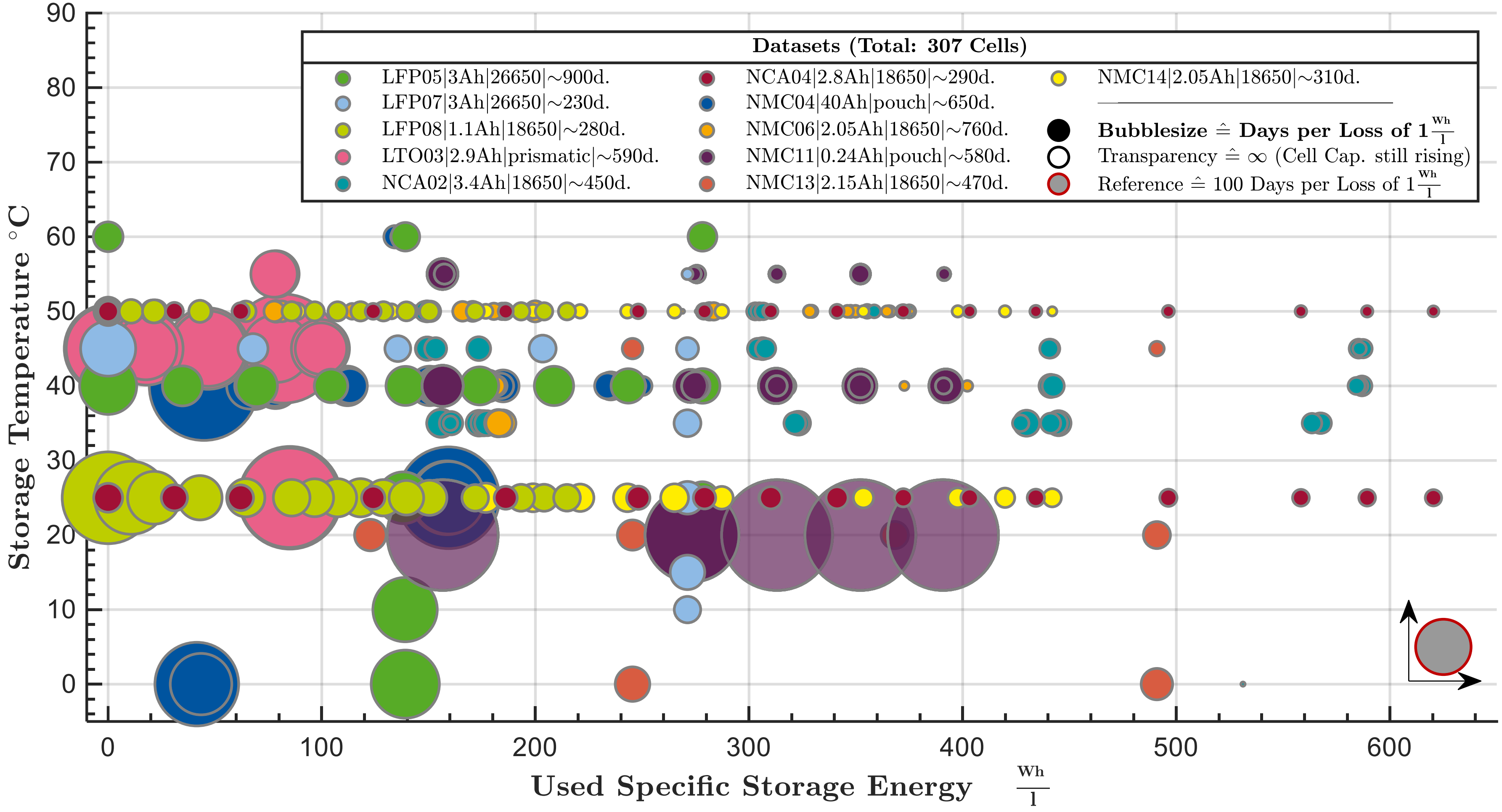
Datasets (Total: 307 Cells)
LFP05|3Ah|26650|~900d.
LFP07|3Ah|26650|~230d.
LFP08|1.1Ah|18650|~280d.
LTO03|2.9Ah|prismatic|~590d.
NCA02|3.4Ah|18650|~450d.
NCA04|2.8Ah|18650|~290d.
NMC04|40Ah|pouch|~650d.
NMC06|2.05Ah|18650|~760d.
NMC11|0.24Ah|pouch|~580d.
NMC13|2.15Ah|18650|~470d.
NMC14|2.05Ah|18650|~310d.
Bubblesize ≙ Days per Loss of 1 Wh/l
Transparency ≙ ∞ (Cell Cap. still rising)
Reference ≙ 100 Days per Loss of 1 Wh/l
Storage Temperature °C
Used Specific Storage Energy Wh/l
90
80
70
60
50
40
30
20
10
0
0
100
200
300
400
500
600